Article

A self-regulatory cell-wall-sensing module at cell edges controls plant growth

Liam Elliott[1,2], Monika Kalde[1], Ann-Kathrin Schürholz[3], Xinyu Zhang[1,2], Sebastian Wolf[3,4], Ian Moore[1,5] & Charlotte Kirchhelle [1,2] ✉

Morphogenesis of multicellular organs requires coordination of cellular growth. In plants, cell growth is determined by turgor pressure and the mechanical properties of the cell wall, which also glues cells together. Because plants have to integrate tissue-scale mechanical stresses arising through growth in a fixed tissue topology, they need to monitor cell wall mechanical status and adapt growth accordingly. Molecular factors have been identified, but whether cell geometry contributes to wall sensing is unknown. Here we propose that plant cell edges act as cell-wall-sensing domains during growth. We describe two Receptor-Like Proteins, RLP4 and RLP4-L1, which occupy a unique polarity domain at cell edges established through a targeted secretory transport pathway. We show that RLP4s associate with the cell wall at edges via their extracellular domain, respond to changes in cell wall mechanics and contribute to directional growth control in *Arabidopsis*.

To develop defined organ shapes, adjacent cells need to coordinate their 3D growth. This can occur through tissue-scale organizing cues (morphogen gradients or stress fields), but at the local scale, heterogeneities in cellular growth can cause mechanical conflicts. In animal systems, such local conflicts can be relaxed through changes in tissue topology. In plants, cells are surrounded by a shared cell wall and cannot move relative to each other. Within the confines of this fixed tissue topology, mechanical conflicts have to be otherwise resolved.

Plant cell growth is driven by non-directional turgor pressure, which is translated into directional growth through construction and modification of a pecto-cellulosic cell wall with heterogeneous biochemical and mechanical properties[1,2]. Plants control growth direction primarily through oriented deposition of cellulose microfibrils of high tensile strength, which constrain growth parallel to their net orientation[3] and are locally reinforced through interactions with hemicelluloses[4]. Pectins influence cell wall porosity but can also contribute to differential extensibility of the cell wall[5–7]. Despite their distinct structures and mechanical properties, the loss of specific cell wall components can be compensated by others. For example, pectins assume a more prominent load-bearing role in plant cell walls

lacking the hemicellulose xyloglucan[8]. This implies that plant cells can perceive changes in their cell wall status and adapt their cell wall biogenesis accordingly. Several cell surface receptor families, including Wall-Associated Kinases (WAKs), *Catharanthus roseus* Receptor-Like Kinase 1-Likes (CrRLK1Ls) and Receptor-Like Proteins (RLPs), have been linked to cell wall sensing[9–14].

Some of these receptors can directly interact with cell wall carbohydrates[6,15,16], while in other cases, association with proteinaceous binding partners is required for downstream signalling events[17–20]. Despite the identification of such ligands, the role of these cell-wall-sensing systems in the continuous assembly and modification of the cell wall required during growth is not well understood. One reason for this may be a lack of appreciation of the spatial context (that is, the 3D geometry of the cell) in which such signals are perceived and translated into cell wall biogenesis.

Here we describe two *Arabidopsis thaliana* RLPs, RLP4 and RLP4-L1, that occupy a unique subcellular domain in the plasma membrane (PM) of growing cells: the geometric edges (where two faces of a polyhedral cell meet in a 1D line). We show that at the cell surface, RLP4s associate with the cell wall and respond to mechanical stimuli. We also

[1]Department of Plant Sciences, University of Oxford, Oxford, UK. [2]Laboratoire Reproduction et Développement des Plantes, Université Lyon 1, ENS de Lyon, CNRS, INRAE, Lyon, France. [3]Centre for Organismal Studies, University of Heidelberg, Heidelberg, Germany. [4]Center for Plant Molecular Biology, University of Tübingen, Tübingen, Germany. [5]Deceased: Ian Moore. ✉e-mail: charlotte.kirchhelle@ens-lyon.fr
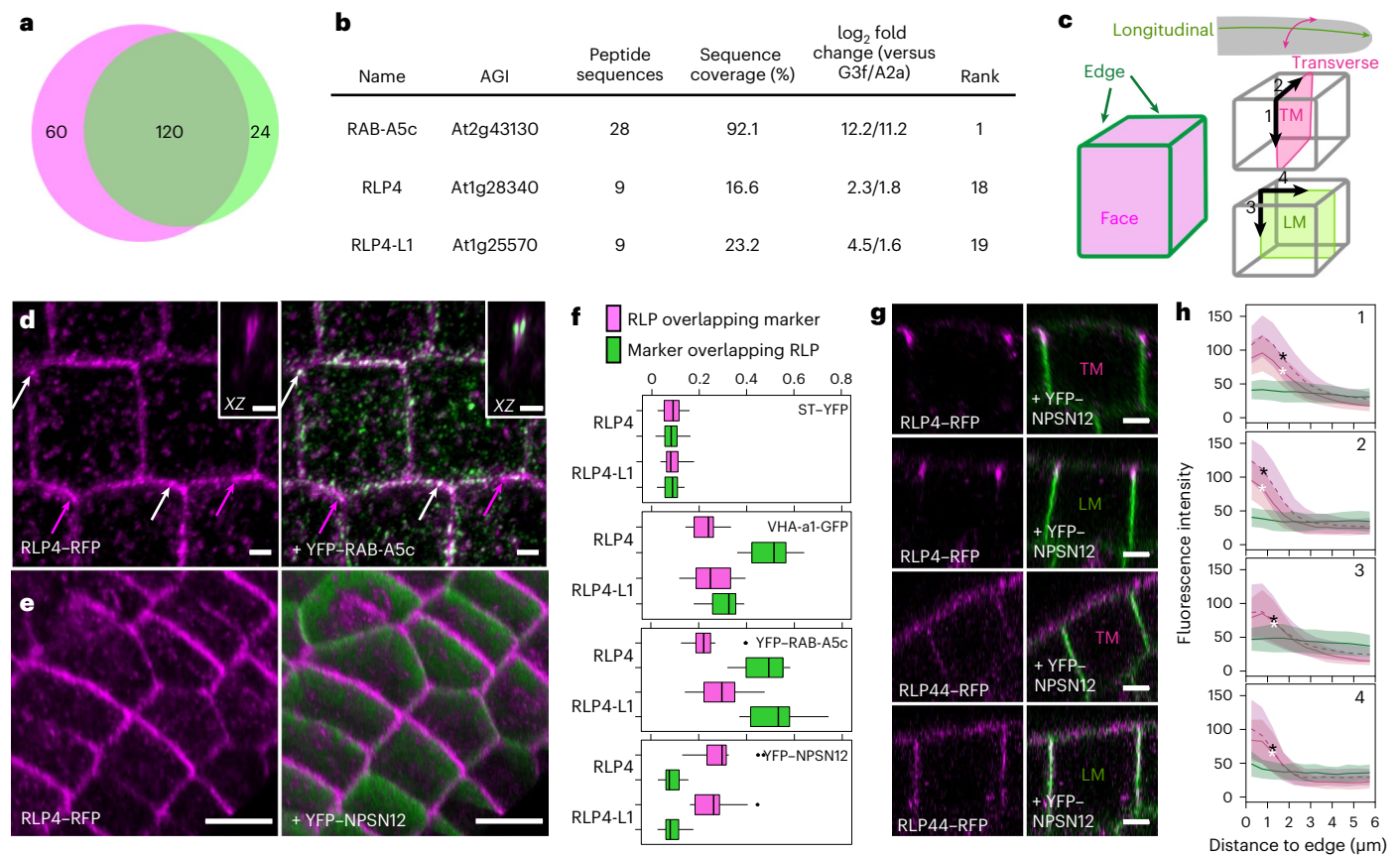
Fig. 1 | RLP4s are edge-polarized at the PM. a, Proteins enriched in the YFP–RAB-A5c interactome compared with YFP–RAB-A2a (magenta) and YFP–RAB-G3f (green). **b**, Ranking for RLP4s from the comparative proteomics approach. **c**, Schematic depiction of cell edges and midplane sections in lateral root epidermal meristem cells. TM, transverse midplane; LM, longitudinal midplane. **d**, Confocal laser scanning microscopy (CLSM) maximum-intensity projection of lateral root epidermal meristem cells co-expressing *pRLP4::RLP4–RFP* and YFP–RAB-A5c. The insets show *XZ* orthogonal sections at a cell edge. The experiments were conducted at least five times independently; representative images are shown. **e**, MorphographX snapshot of a lateral root meristem co-expressing *pUBQ10::RLP4–RFP* and YFP–NPSN12. **f**, Manders's colocalization coefficients showing the fraction of RLP4s–RFP colocalizing with different membrane markers. CLSM stacks from three or four lateral root meristems were subdivided into non-overlapping substacks of 25 μm × 25 μm ('regions'). *N* = 13 regions from four lateral roots (RLP4–RFP/VHA-a1–GFP) or 14 regions from three or four roots

(all other combinations). See Methods for an explanation of the box plots. **g**, CLSM *XZ/YZ* projections representing TM and LM midplane sections through epidermal meristematic lateral root cells co-expressing *pUBQ10::RLP4–RFP* or *pUBQ10::RLP44–RFP* and YFP–NPSN12. The experiments were conducted at least five times independently; representative images are shown. **h**, Quantification of fluorescence intensity of RLP4–RFP (red), RLP4-L1–RFP (magenta, dashed line) and RLP44–RFP (green) with increasing distance from the cell edge along the trajectories labelled 1–4 in **c**. The lines indicate average fluorescence intensity in midplane sections with increasing distance from the edge. *N* for RLP4–RFP along trajectories 1–4 are 108, 123, 82 and 151, respectively. *N* for RLP4-L1–RFP for trajectories 1–4 are 103, 121, 92 and 162, respectively. The shaded areas indicate ±1 s.d. The asterisks indicate the distance from the cell edge at which RLP4–RFP (white asterisks) or RLP4-L1–RFP (black asterisks) signal intensity became significantly lower than at the edge (one-way ANOVA and post-hoc Tukey test, *P* < 0.05). Scale bars, 1 μm (**a**), 5 μm (**g**) or 10 μm (**e**).

show that surface-localized RLP4s contribute to directional growth control in *Arabidopsis* lateral roots through organizing edge-directed intracellular transport. On the basis of these data, we propose a mechanistic model for the translation of cell wall mechanical feedback into 3D growth through cell edges.
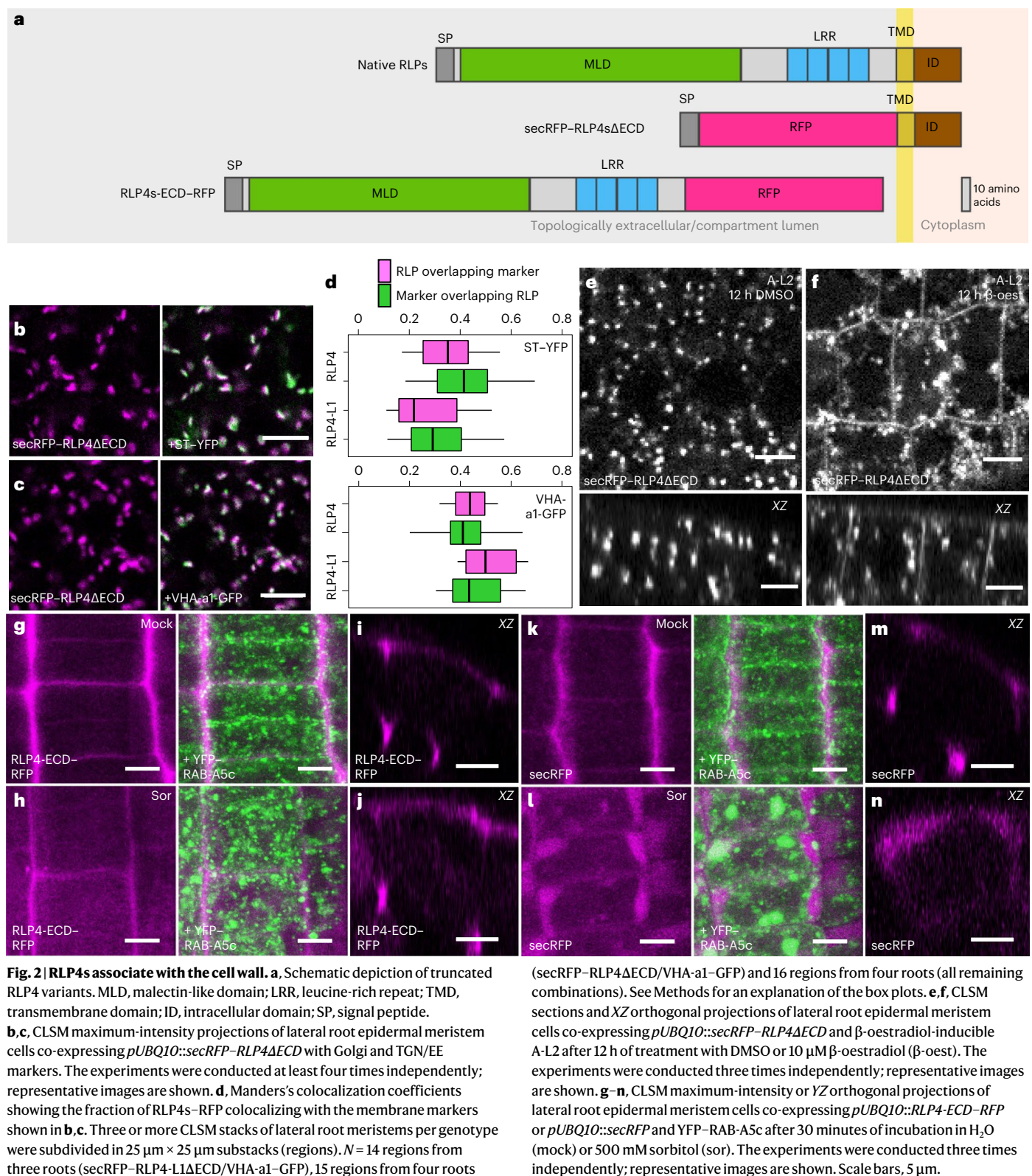
Results

Two RLPs localize to plant cell edges

The plant-specific GTPase RAB-A5c mediates a transport pathway targeted to cell edges that is required for directional growth in *Arabidopsis* lateral roots[21]. We performed co-immunoprecipitation coupled with label-free semi-quantitative mass spectrometry against YFP–RAB-A5c[21] to identify interactors of RAB-A5c. To separate generic Rab interactors from those specific to RAB-A5c, we identified proteins significantly enriched in the YFP–RAB-A5c interactome compared with the interactomes of two related Rab GTPases: the late endosome/tonoplast-localized YFP–RAB-G3f[22] and the *trans*-Golgi network/early endosome (TGN/EE)-localized YFP–RAB-A2a[23] (Supplementary Data 1,

Fig. 1a and Extended Data Fig. 1a,b). In the top 20 candidates identified in this approach, we found two related proteins: RECEPTOR-LIKE PROTEIN4 (RLP4)[24] and its closest relative in *Arabidopsis*, At1g25570, which we refer to as RECEPTOR-LIKE PROTEIN 4-LIKE1 (RLP4-L1) (Fig. 1b).

Fluorescently tagged versions of RLP4 and RLP4-L1 (henceforth collectively referred to as RLP4s) under the control of their native promoters (*pRLP4s::RLP4s–GFP*) were functional (see the details below and in Fig. 4g and Extended Data Fig. 6e,f) and were highly expressed in growing tissues of the root and shoot (Extended Data Fig. 2a–l). Similarly to what has previously been described for *pRAB-A5c::YFP–RAB-A5c*[21], expression in lateral roots was highest in epidermal meristem cells and was progressively reduced in differentiating cells (Extended Data Fig. 2m).

At the cellular level, RLP4s expressed under either their native (*pRLP4s::RLP4s–RFP/ pRLP4s::RLP4s–GFP*) or the UBIQUITIN10 promoter (*pUBQ10::RLP4s–RFP*) labelled intracellular punctae as well as the cell periphery (Fig. 1d and Extended Data Fig. 1c–j). Quantitative colocalization analyses with a series of endomembrane

Fig. 2 | RLP4s associate with the cell wall. a, Schematic depiction of truncated RLP4 variants. MLD, malectin-like domain; LRR, leucine-rich repeat; TMD, transmembrane domain; ID, intracellular domain; SP, signal peptide. **b,c**, CLSM maximum-intensity projections of lateral root epidermal meristem cells co-expressing *pUBQ10::secRFP–RLP4ΔECD* with Golgi and TGN/EE markers. The experiments were conducted at least four times independently; representative images are shown. **d**, Manders's colocalization coefficients showing the fraction of RLP4s–RFP colocalizing with the membrane markers shown in **b,c**. Three or more CLSM stacks of lateral root meristems per genotype were subdivided in 25 μm × 25 μm substacks (regions). *N* = 14 regions from three roots (secRFP–RLP4-L1ΔECD/VHA-a1–GFP), 15 regions from four roots (secRFP–RLP4ΔECD/VHA-a1–GFP) and 16 regions from four roots (all remaining combinations). See Methods for an explanation of the box plots. **e,f**, CLSM sections and *XZ* orthogonal projections of lateral root epidermal meristem cells co-expressing *pUBQ10::secRFP–RLP4ΔECD* and β-oestradiol-inducible A-L2 after 12 h of treatment with DMSO or 10 μM β-oestradiol (β-oest). The experiments were conducted three times independently; representative images are shown. **g–n**, CLSM maximum-intensity or *YZ* orthogonal projections of lateral root epidermal meristem cells co-expressing *pUBQ10::RLP4-ECD–RFP* or *pUBQ10::secRFP* and YFP–RAB-A5c after 30 minutes of incubation in H$_2$O (mock) or 500 mM sorbitol (sor). The experiments were conducted three times independently; representative images are shown. Scale bars, 5 μm.

compartment markers demonstrated that RLP4s–RFP localized in similar proportions to RAB-A5c edge compartments, the TGN/EE, and the PM, while labelling the Golgi to a lesser extent (Fig. 1e,f and Extended Data Fig. 3a–h). RLP4s–RFP were confined to a subdomain of the PM, which was apparent in our colocalization analyses (Manders's colocalization coefficient, 0.09 ± 0.04 in both cases) as well as in orthogonal or 3D projections of confocal stacks, in which

RLP4s–RFP were strikingly confined to cell edges (Fig. 1d,e,g,h and Extended Data Figs. 1e,f and 3i–l). This pattern differed significantly from that of RLP44–RFP, a related PM-localized RLP[25] that does not label edge compartments (Fig. 1g,h). We have previously proposed that RAB-A5c mediates a secretory pathway from the TGN/EE to the PM at cell edges on the basis of the localization of nucleotide-free and constitutively active RAB-A5c variants to these compartments[21].

To test whether RLP4s–RFP are a cargo of RAB-A5c-mediated transport, we overexpressed dominant-negative RAB-A5c-N125I, which disrupts RAB-A5c function without inhibiting bulk secretory traffic[21]. In the presence of RAB-A5c-N125I, RLP4s–RFP were depleted from cell edge compartments and the PM (Extended Data Fig. 3m–p). We conclude that RLP4s reach the cell edge domain as cargos of RAB-A5c-mediated edge-directed transport, where they define a unique polarity domain.

RLP4s interact with the cell wall at edges

RLP4s are predicted to contain a short intracellular domain, a transmembrane domain and an extracellular domain (ECD) containing leucine-rich repeats as well as a putatively carbohydrate-binding malectin-like domain also found in some CrRLK1Ls[24] (Fig. 2a). The ECDs of other RLPs can interact with extracellular proteinaceous ligands or the cell wall[26], whereas the intracellular domain is expected to interact with intracellular trafficking machinery.

To functionally characterize the ECD of RLP4s, we expressed RLP4s variants lacking their ECD fused to a secreted version of RFP (secRFP), targeting them to the secretory pathway (*pUBQ10::secRFP–RLP4sΔECD*; Fig. 2a). secRFP–RLP4sΔECD exclusively localized to intracellular compartments and did not label edge compartments or the PM (Fig. 2b,c and Extended Data Fig. 4a–d), while colocalization with Golgi and TGN/EE markers was significantly increased in comparison with full-length RLP4s–RFP (Fig. 2d versus Fig. 1f; *P* < 0.001, analysis of variance (ANOVA) and post-hoc Tukey test).

By contrast, full-length RLP4s with the equivalent amino-terminal tag (*pUBQ10::secRFP–RLP4s*) localized in the same pattern as carboxy-terminally tagged RLP4s (Extended Data Fig. 1g,h), suggesting that the N-terminal position of the tag did not interfere with protein transport. We hypothesized that secRFP–RLP4sΔECD may be secreted but undergo rapid endocytosis, preventing the accumulation of detectable levels at the PM. Consistent with this hypothesis, conditional overexpression of the clathrin uncoating factor AUXILIN-LIKE2 (A-L2), which causes specific inhibition of clathrin-mediated endocytosis[27], resulted in partial relocalization of secRFP–RLP4sΔECD to the PM (Fig. 2e,f and Extended Data Fig. 4e,f).

We also expressed the RLP4s-ECD fused to RFP (*pUBQ10::RLP4s-ECD–RFP*). These truncations were secreted to the cell wall, with the strongest signal emanating from cell edges (Fig. 2g,i and Extended Data Fig. 4g,i). This pattern was also observed when secRFP was expressed on its own (*pUBQ10::secRFP*; Fig. 2k,m) and presumably reflects an inherent property of the cell wall rather than specific targeting of the protein to cell edges. In line with this interpretation, RLP4-ECD–RFP accumulated in the lobe regions of cotyledon pavement cells, where cell walls were thickest (Extended Data Fig. 4k). However, when we treated cells with 500 mM sorbitol for 30 min to plasmolyse them, secRFP flooded into the gap between the retracting protoplast

and the cell wall (Fig. 2l,n), whereas RLP4s-ECD–RFP remained at the cell wall (Fig. 2h,j and Extended Data Fig. 4h,j). Taken together, our data show that the RLP4s-ECD can associate with the cell wall and are stabilized at the cell surface through this interaction.

RLP4s respond to changes in cell wall mechanics

Considering their interaction with the cell wall, we hypothesized that RLP4s may act as cell wall sensors during growth. To test whether RLP4s are responsive to changes in cell wall mechanical status, we treated plants expressing RLP4s–RFP with isoxaben (IXB), an inhibitor of cellulose biosynthesis[28]. After three days of treatment with 2.5 nM IXB, RLP4–RFP was depleted from the PM and RAB-A5c-labelled compartments, whereas accumulation at the TGN/EE significantly increased (Fig. 3a–c). We observed a qualitatively similar albeit slightly weaker shift in localization from the PM towards intracellular compartments for RLP4-L1–RFP (Extended Data Fig. 5a–h).

We also noticed that YFP–RAB-A5c compartments were depleted from cell edges in IXB-treated roots (Fig. 3a,b), indicating that edge-directed transport itself was perturbed during IXB treatment. IXB acts through inhibiting the transport of cellulose synthase complexes to the PM[29]. This mode of action is believed to be due to specific interactions of IXB with the cellulose synthase subunits CESA3 and CESA6 (refs. 28,30), and trafficking of the PM-localized YFP–NPSN12 was not affected by IXB in our experiments (Extended Data Fig. 4c,d,g,h). However, IXB has been reported to perturb intracellular trafficking of the *endo*-1,4-β-*d*-glucanase KORRIGAN1 (ref. 31), and we could not exclude the possibility that the depletion of RLP4s from the cell surface was driven primarily by a perturbation of RLP4s transport to the cell surface rather than a direct response of RLP4s to cell wall status. To distinguish between the effects of IXB on RAB-A5c/RLP4s trafficking and those on surface retention of RLP4s, we employed an alternative strategy to perturb cell wall mechanical status that did not rely on long treatment periods.

We ablated small groups of cells with a microneedle to induce instantaneous local changes in cell geometry (Fig. 3d) and alterations of cell wall stress patterns surrounding the wound site[32]. We imaged lateral roots within five minutes before and after ablation, allowing us to follow the dynamics of RLP4s in response to mechanical perturbations with much higher temporal resolution. In these experiments, RLP4–RFP was significantly depleted from cell edges in the vicinity of ablations in comparison with the PM marker YFP–NPSN12 (Fig. 3e–g). To distinguish whether the loss of RLP4–RFP signal was due to loss of secretion or increased endocytosis of RLP4–RFP after ablation, we also conducted ablations in the presence of inducibly expressed A-L2 to inhibit endocytosis (Fig. 3h–p). After 16 h of induction, the RLP4–RFP pattern at cell edges was indistinguishable in A-L2-expressing and A-L2-non-expressing roots (Fig. 3h,j,l). However, after ablation, RLP4–RFP intensity at cell edges was significantly higher in

Fig. 3 | RLP4 responds to changes in cell wall mechanical status. a,b, CLSM maximum-intensity projections of lateral root epidermal meristems coexpressing *pUBQ10::RLP4–RFP* and *pRAB-A5c::YFP–RAB-A5c* after three days of treatment with 2.5 nM IXB or DMSO. **c**, Manders's colocalization coefficients between RLP4s–RFP and various membrane markers with or without IXB as shown in **a,b**. *N* = 14 regions from two roots (VHA-a1–GFP DMSO and YFP–RAB-A5c DMSO), 15 regions from two roots (VHA-A1–GFP IXB), 16 regions from two roots (YFP–RAB-A5c IXB) or 17 regions from three roots (the remaining combinations). **P* < 0.05; ****P* < 0.001 (ANOVA with post-hoc Tukey test). See Methods for an explanation of the box plots. **d–f**, CLSM maximum-intensity projections of a lateral root epidermal meristem coexpressing RLP4–RFP and YFP–NPSN12 before and immediately after cell ablation (asterisks). **g**, Fluorescence intensity ratio of RLP4–RFP and YFP–NPSN12 after and before ablation on transverse midplane sections of epidermal meristem cells undergoing deformation after ablation like those shown in **d–f**. The lines indicate average values (*N* ≥ 62 edges from five roots), and the shaded areas show ±1 s.d. The asterisks indicate significant differences between RLP4–RFP and

YFP–NPSN12 (one-way ANOVA and post-hoc Tukey test; ****P* < 0.001). **h–k**, *XZ* projections showing the same anticlinal cell edges of lateral roots co-expressing *pUBQ10::RLP4–RFP*, YFP–NPSN12 and β-oestradiol-inducible A-L2 after 16 h of treatment with DMSO (**h,i**) or 10 μM β-oestradiol (**j,k**) before (**h,j**) and after (**i,k**) microneedle ablation. **l**, Fluorescence intensity of RLP4–RFP before and after ablation on midplane sections of epidermal meristem cells like those in **h–k**. The lines indicate average fluorescence intensity (*N* = 24 (DMSO) and *N* = 32 (β-oestradiol) edges from three roots, respectively), and the shaded areas show ±1 s.d. The asterisks indicate significant differences in RLP4–RFP intensity between DMSO and β-oestradiol treatments (one-way ANOVA and post-hoc Tukey test; ****P* < 0.001). Before the ablation, there was no significant difference in RLP4–RFP intensity between treatments. **m–p**, CLSM maximum-intensity projections of lateral root epidermal meristem cells coexpressing RLP4–RFP and YFP–RAB-A5c in the absence (**m,n**) or presence (**o,p**) of inducible A-L2 before (**m,o**) and immediately after cell ablation (**n,p**; asterisks). Note that RLP4–RFP and YFP–RAB-A5c show increased retention at the cell edge in the presence of A-L2 (arrows). Scale bars, 10 μm (**d–f**), 5 μm (**a,b,m–p**) or 2 μm (**h–k**).
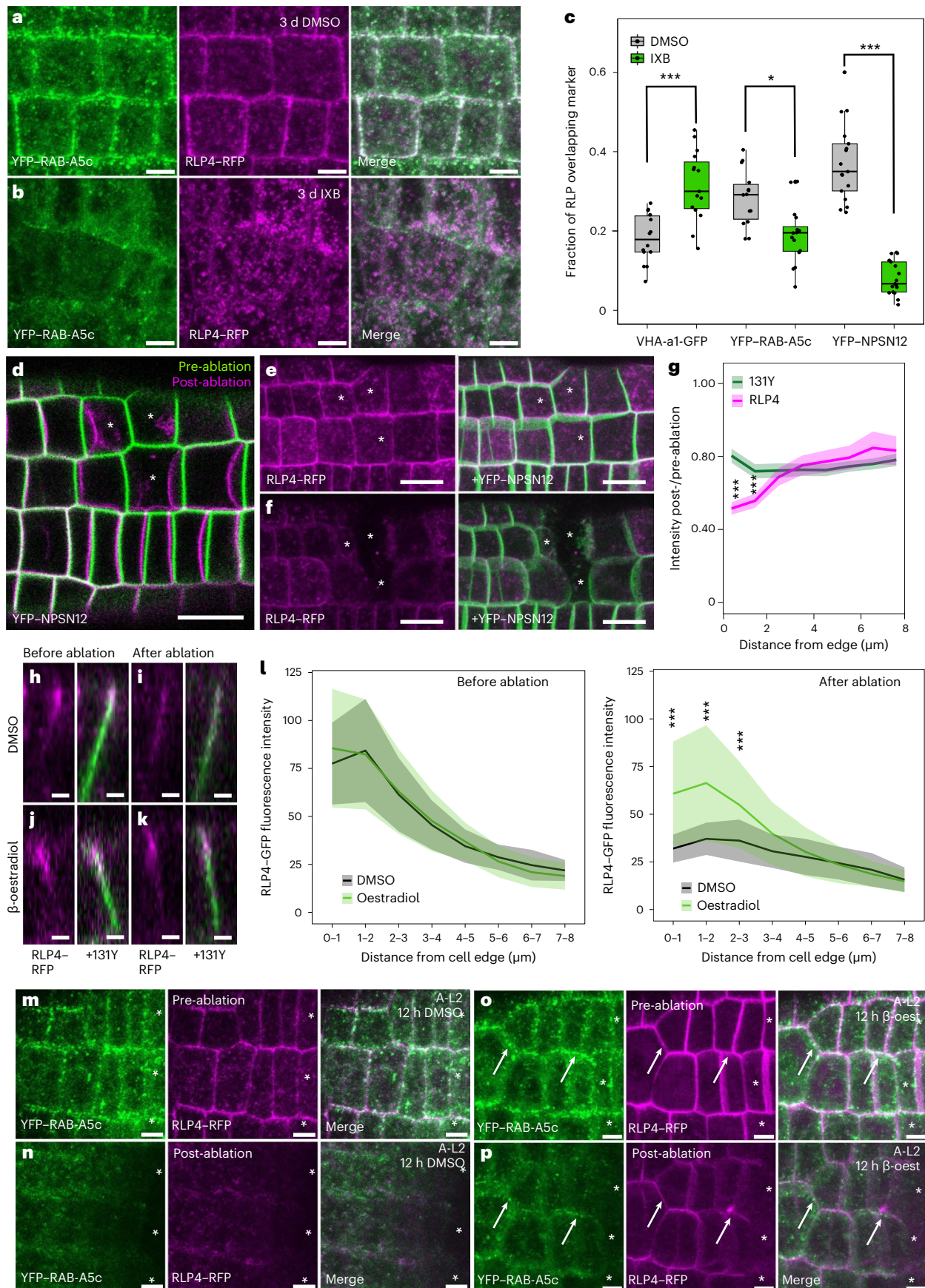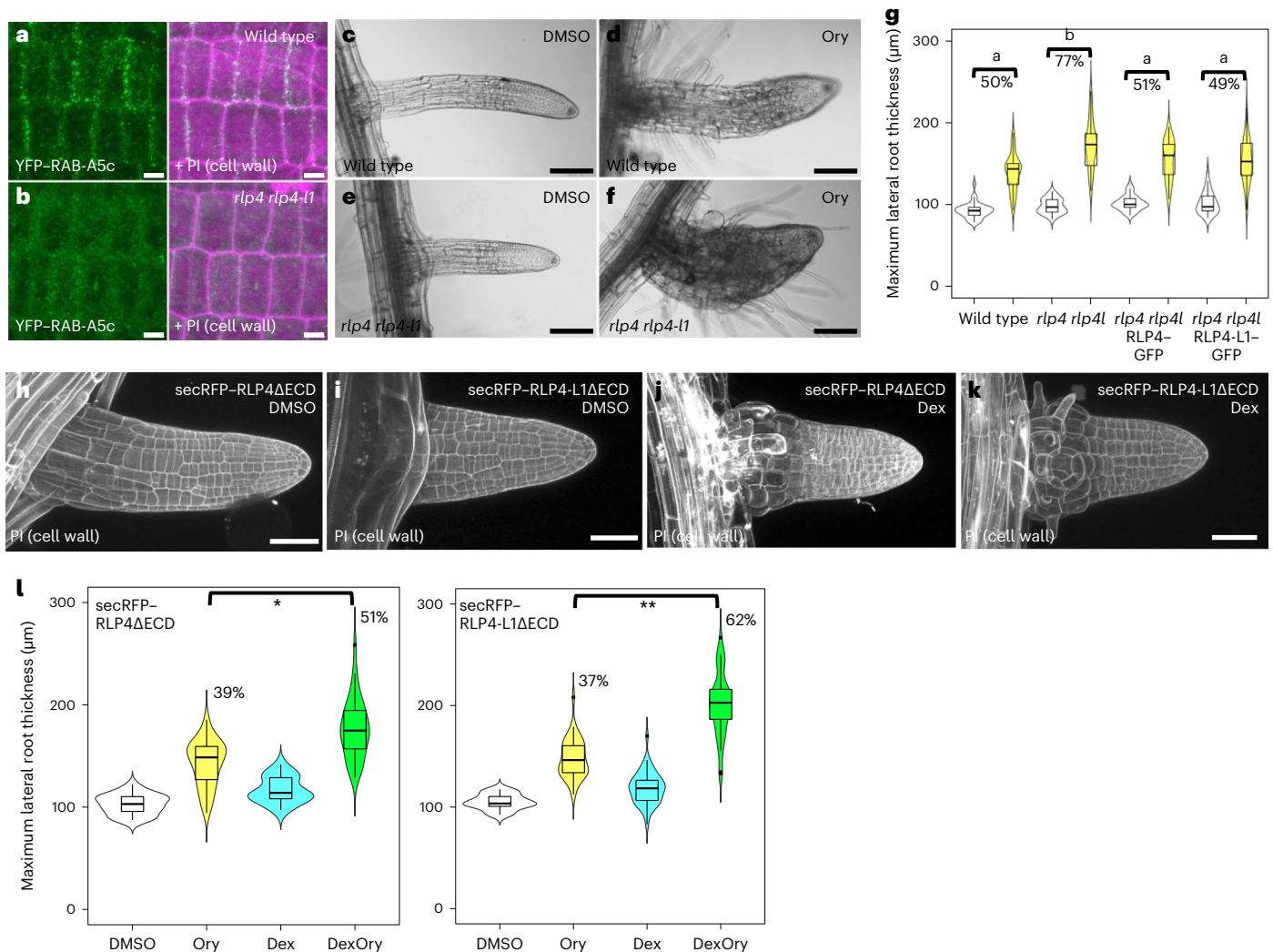
Fig. 4 | RLP4s contribute to directional growth control. a,b, CLSM maximum-intensity projections of lateral root epidermal meristem cells expressing YFP–RAB-A5c in the wild-type (**a**) or *rlp4 rlp4-l1* (**b**) background. The cell wall was stained with propidium iodide (PI). Representative images from one of three independent experiments are shown. **c–f,** Lateral roots from wild-type and *rlp4 rlp4-l1* plants grown for three days on DMSO or 250 nM oryzalin (Ory). **g,** Violin plots of the mean maximum diameter of lateral roots from plants grown for three days on DMSO or 250 nM oryzalin like those shown in **c–f** or S6F. *N* for DMSO and oryzalin for each genotype were 37 and 34 (wild type), 35 and 42 (*rlp4 rlp4-l1*), 36 and 37 (*rlp4 rlp4-l1 pRLP4::RLP4–GFP*) and 33 and 38 (*rlp4 rlp4-l1 pRLP4-L1::RLP4-L1–GFP*). The difference in diameter (%) between DMSO and oryzalin treatments for each genotype is noted above the respective columns. Relative diameter increased significantly more in response to oryzalin treatment in *rlp4 rlp4-l1* than in the wild type (*P* = 0.000007), which could be fully rescued by introducing *pRLP4::RLP4–GFP* (*P* = 1) or *pRLP4-L1::RLP4-L1–GFP* (*P* = 1) into the *rlp4 rlp4-l1* background. The letters indicate significant differences in

relative root diameter increase (*P* < 0.05; two-way ANOVA and post-hoc Tukey test). Representative results from one of three independent experiments are shown. See Methods for an explanation of the violin plots. **h–k,** CLSM maximum-intensity projections of lateral roots expressing *pRPS5a»Dex»secRFP–RLP4sΔECD* three days after transfer to DMSO or 10 μM Dex. The cell wall was stained with propidium iodide. **l,** Violin plots of the mean maximum diameter of lateral roots from seedlings expressing *pRPS5a»Dex»secRFP–RLP4sΔECD* grown on 250 nM oryzalin and/or 1 μM Dex or the equivalent quantity of DMSO for three days. *N* for DMSO, oryzalin, Dex and Dex oryzalin, respectively, were 30, 39, 18 and 34 (*RLP4ΔECD*); and 27, 37, 28 and 34 (*RLP4-L1ΔECD*). Relative diameter increases were significantly different for oryzalin treatments in the presence versus absence of Dex (**P* = 0.038, ***P* = 0.012; two-way ANOVA and post-hoc Tukey test). Representative results from one of three independent experiments are shown. See Methods for an explanation of the violin plots. Scale bars, 5 μm (**a,b**), 50 μm (**h–k**) or 100 μm (**c–f**).

A-L2-expressing roots (Fig. 3i,k,l), indicating that the observed reduction in RLP4–RFP under control conditions depended on endocytosis rather than secretion.

We conclude that RLP4s–RFP abundance at the surface changes in response to cell wall mechanical and/or biochemical status through enhanced endocytosis.

RLP4s are required for RAB-A5c patterning and growth control

We also investigated localization patterns of YFP–RAB-A5c in ablation experiments and found that YFP–RAB-A5c was also lost from cell

edges after ablations (Fig. 3m,n). When we conducted ablations in plants overexpressing A-L2, more YFP–RAB-A5c-labelled compartments persisted at cell edges in cells close to ablation sites (Fig. 3o,p), raising the question of whether RLP4s are directly involved in RAB-A5c recruitment to cell edges.

To test this hypothesis, we used CRISPR–Cas9 to obtain transcriptional null *rlp4 rlp4-l1* mutants. In *rlp4 rlp4-l1* mutants, YFP–RAB-A5c was depleted from cell edges but not from cell plates (Fig. 4a,b and Extended Data Fig. 6a,b), indicating that RLP4s are required for RAB-A5c localization to cell edges during interphase. While the inhibition of RAB-A5c function causes severe growth defects[21],
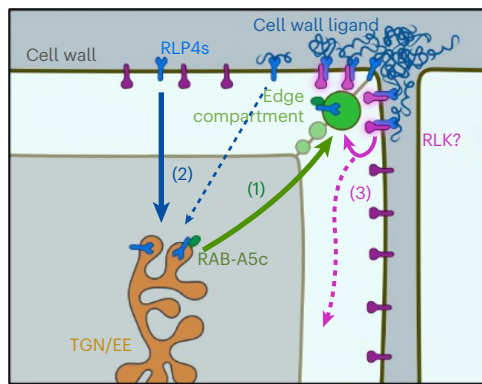
Fig. 5 | A hypothetical model for a self-regulating edge-based cell-wall-sensing module. (1) RLP4s are transported from the TGN/EE to the cell edge through RAB-A5c-mediated trafficking. (2) RLP4s are stabilized at the cell surface though interaction with a cell wall ligand, and the association of RLP4s with the cell wall is sensitive to changes in cell wall mechanical status. RLP4s that are not cell wall associated are endocytosed, thus providing a concentration-based system for cell wall sensing. (3) Surface-localized RLP4s associate with an as-yet-unidentified RLK to form a signalling module, among whose targets is RAB-A5c-mediated transport itself.

rlp4, *rlp4-l1* and *rlp4 rlp4-l1* were phenotypically indistinguishable from wild-type plants in standard growth conditions (Extended Data Fig. 6c,d). We have previously demonstrated that growth defects caused by the inhibition of RAB-A5c can be partially compensated through increased anisotropy of microtubule arrays, rendering RAB-A5c-N125I plants hypersensitive to the microtubule-depolymerizing drug oryzalin[33]. To test whether similar compensatory mechanisms may explain the lack of growth defects in *rlp4 rlp4-l1* plants, we treated wild-type and *rlp4 rlp4-l1* plants with oryzalin. We found significantly higher lateral root swelling in *rlp4 rlp4-l1* than in wild-type lateral roots (Fig. 4c–g; 77% versus 50%, respectively), phenocopying oryzalin-treated RAB-A5c-N125I plants[33]. This phenotype was suppressed by the introduction of *pRLP4::RLP4–GFP* or *pRLP4-L1::RLP4-L1–GFP* into the *rlp4 rlp4-l1* background, indicating that tagged versions of RLP4s were functional (Fig. 4g and Extended Data Fig. 6f). Interestingly, expression of the same protein variants in the wild-type background caused a significant increase in sensitivity to oryzalin compared with wild-type plants, although not to the same extent as *rlp4 rlp4-l1* (Extended Data Fig. 6e,f). This suggests that plants are sensitive to the level of RLP4s, and overexpression as well as lack of RLP4s can lead to reduced growth robustness.

We also aimed to conditionally disrupt RLP4s function and hypothesized that the overexpression of secRFP–RLP4sΔECD protein variants, which predominantly localized to the Golgi and TGN/EE (Fig. 2b–d and Extended Data Fig. 4a–d), may be used to disrupt the transport of wild-type RLP4s through competitive titration of intracellular trafficking machinery. We expressed these protein variants under the control of the dexamethasone (Dex)-inducible pOp/LhGR system[34] (At*RPS5a»DEX»secRFP–RLP4sΔECD*) and found that secRFP–RLP4sΔECD overexpression strongly reduced the fluorescence of co-expressed *pRLP4s::RLP4s–GFP* at cell edges as well as intracellular compartments (Extended Data Fig. 7a–h). When induced from germination, secRFP–RLP4sΔECD caused growth defects reminiscent of those found in the roots and shoots of plants expressing RAB-A5c-N125I in 13/29 and 17/27 independent transgenic lines, respectively (Extended Data Fig. 7i).

When seven-day-old seedlings grown under non-inducing conditions were transferred to Dex for three days, lateral root morphology was strongly perturbed in secRFP–RLP4sΔECD plants (Fig. 4h–k). We have previously shown that RAB-A5c function is required for directional growth during interphase as well as cytokinesis, the latter of

which is a function shared with other Rab-A GTPases[21]. By contrast, we observed no cytokinesis defects in At*RPS5a»DEX»secRFP–RLP4sΔECD* lines, indicating that RLP4s act specifically during interphase growth. Furthermore, At*RPS5a»DEX»secRFP–RLP4sΔECD* lines were hypersensitive to oryzalin (Fig. 4l and Extended Data Fig. 7j,k), phenocopying At*RPS5a»DEX»RAB-A5c*[N125I] and *rlp4 rlp4-l1*. We conclude that RLP4s control directional growth during interphase through tuning the delivery of RAB-A5c compartments to cell edges.

Discussion

In this study, we identified and characterized two cell-wall-associated RLPs, RLP4 and RLP4-L1, which localize to cell edges, respond to changes in cell wall mechanics and are functionally linked to directional growth control. In growing tissues, 3D cellular growth is coordinated in different developmental zones but can vary substantially in neighbouring cells[33,35]. However, growth at shared 2D cell faces must be strictly synchronized to maintain tissue integrity. Even cell faces that are not shared (that is, at the outer organ surface) need to grow at appropriate rates to prevent cell bulging or rupture. 1D cell edges delimit cell faces in all directions, and requisite cell growth at any particular cell face can be considered as the product of integration of growth vectors along all edges delimiting the face. This implies that broader 2D and 3D growth patterns arise as a consequence of 1D growth control at cell edges.

We and others have previously shown that cell edges are sites at which directional growth can be controlled[21,36], but on the basis of the data presented here, we now propose cell edges simultaneously act as cell-wall-sensing domains through which cell wall mechanical status can be perceived and integrated into directional growth control (Fig. 5). We propose that (1) RAB-A5c mediates the delivery of RLP4s to the cell edge domain, where RLP4s associate with a cell wall ligand via their ECD; and (2) RLP4s abundance at the cell surface is constantly adapted through the removal of non-cell-wall-associated RLP4s through endocytosis, which allows rapid response to changes in cell wall status. RLP4s lack an intracellular kinase domain to initiate a downstream signalling cascade, and we currently do not know any interaction partners at the cell surface. However, other PM-localized RLPs interact with RLKs to form signalling modules that initiate intracellular signal cascades[25,37,38]. We therefore propose (3) a similar mode of action for RLP4s, which may act as a scaffold for an edge-based signalling hub whose activity can be controlled through RLP4s abundance at the edge. While we have not yet identified a direct target of such a module, our data show that RAB-A5c is among the downstream effectors of RLP4s, thus forming a positive feedback loop of edge-based growth control. This model can explain how cell wall mechanical status can be integrated into directional growth control through 1D cell edges.

We have developed this framework of edge-based growth control in plant tissues. However, there are many conceptual parallels to epidermal tissues in animals. In such tissues, tricellular junctions (anticlinal edges) have been implicated in responses to mechanical stimuli and also accumulate components of the JNK and Hippo growth signalling pathways[39]. This raises the intriguing possibility that growth control mechanisms in multicellular organisms of different lineages converge on 1D cell edges as regulatory domains.

Methods
Plant materials and growth
The *A. thaliana* ecotype Columbia (Col-0) was used throughout. The following transgenic lines used in this study have been described before: *pRAB-A5c::YFP–RAB-A5c*[21], At*RPS5a»Dex»RAB-A5c*[N125I] (ref. 21), *pUBQ10::YFP–NPSN12* (ref. 22), *pUBQ10::YFP–RAB-G3f*[22], *pRAB-A2a::YFP–RAB-A2a*[23], *pVHA-a1::VHA-a1–GFP*[40], *p35S::ST–YFP*[41] and *XVE»AL1/XVE»AL2* (ref. 27).

For the simultaneous targeting of *RLP4* and *RLP4-L1* via CRISPR–Cas9, two suitable sequences for the generation of guide RNAs were

determined using the ChopChop webpage (https://chopchop.cbu.uib.no/) and incorporated into oligonucleotides that also contained an Eco31I recognition site at the 5′ end and a pHEE2E-TRI-specific[42] sequence at the 3′ end. pHEE2E-TRI was used as a template to amplify the two targeting sequences together with the promoter and terminator regions. The amplified PCR product was gel-purified and ligated into Eco31I (BsaI)-digested pHEE2E-TRI. The assembled construct was mobilized in *Agrobacterium tumefaciens* strain GV3101 and used to transform Col-0 plants. T_1 plants were selected on half-strength Murashige and Skoog (MS) medium containing 0.75% phytoagar and 15 µg ml⁻¹ hygromycin. The plates were covered with sheets of paper for four to six days until positive T_1 plants with an elongated hypocotyl could be distinguished and kept for another four days at full light. Around 40 T_1 plants were transferred to soil and analysed for mutations using primers. We isolated a Cas9-free double mutant with single base insertions in both genes (position 264 from ATG for RLP4 and position 363 for RLP4-L1), leading to premature stop codons 14 and 11 exons downstream, respectively.

All plants were grown at 20 °C in a 16 h:8 h day:night cycle. Lateral roots were imaged 8–12 days after germination on upright half-strength MS medium (Sigma Aldrich) plates with 1% w/v sucrose and 0.8% Bacto agar (Appleton Woods) at pH 5.7. For conditional expression using either Dex or β-oestradiol, seedlings were grown for seven days from germination before transfer to half-strength MS medium containing either 10 µM Dex (Sigma Aldrich; diluted from a 10 mM stock in DMSO), 10 µM β-oestradiol (Sigma Aldrich; diluted from 10 mM a stock in DMSO) or an equivalent volume of DMSO solvent for the indicated period. Plasmolysis was performed by immersion of plants in 0.5 M sorbitol solution for 30 minutes. For pharmacological treatments with oryzalin or IXB, seedlings were grown for seven days from germination before transfer to half-strength MS medium containing either 2.5 nM IXB (Sigma Aldrich), 250 nM oryzalin (Sigma Aldrich; diluted from a 10 mM stock in DMSO) or an equivalent volume of DMSO solvent for the indicated period.

The introduction of novel transgenes into plants was performed using *Agrobacterium*-mediated floral dip transformation[43].

Molecular cloning

All genes were amplified by PCR using Phusion High-Fidelity DNA Polymerase (Thermo Fisher Scientific) from genomic DNA isolated from *A. thaliana* ecotype Col-0. *pUBQ10::RLP4/4-L1–RFP*, *pUBQ10::RLP44–RFP* and *pUQ10B::RLP4/4-L1-ECD–RFP* were all generated by cloning the relevant genomic DNA region into pDONR207 (Invitrogen/Thermo Fisher Scientific) using Gateway BP Clonase II Enzyme Mix (Thermo Fisher Scientific) and subsequently into *pUB–RFP–DEST* (9) using Gateway LR Clonase II Enzyme Mix (Thermo Fisher Scientific). For expression of RLP4–RFP and RLP4-L1–RFP from their native promoters, the UBQ10 promoter was removed from *pUB–RFP–DEST* through digestion with restriction endonucleases PspXI and PmeI (New England Biolabs), and the vector was subsequently re-ligated using Klenow polymerase (DNA Polymerase I, Large fragment; New England Biolabs) and T4 DNA ligase (Thermo Fisher Scientific) to generate *pX–DEST–RFP*. The promoter region, 5′ untranslated region and coding region of RLP4 and RLP4-L were then amplified by PCR as single cassettes and cloned into *pDONR207* and eventually *pX–DEST–RFP* as described above. To generate *pUBQ10::secRFP–RLP4s* and *pUBQ10::secRFP–RLP4sΔECD*, the relevant genomic DNA regions were overlapped with *secRFP*[44] and the cassettes cloned into *pENTR/D-TOPO* using a pENTR/D-TOPO Cloning Kit (Thermo Fisher Scientific) and subsequently *pUB–DEST*[45]. For conditional expression of RLP4s and truncated variants using the pOp/LhGR system, transgenes were cloned into *pDONR207* using Gateway BP Clonase II Enzyme Mix (Thermo Fisher Scientific) and subsequently into *pOpIN2–RPS5a*[34] using Gateway LR Clonase II Enzyme Mix (Thermo Fisher Scientific). All constructs were verified by Sanger sequencing (Source Bioscience) and restriction digests.

For molecular cloning, *Escherichia coli* strains DH5α and DB3.1 were used. For *Agrobacterium*-mediated transformation of *Arabidopsis*, constructs were introduced into *Agrobacterium tumefaciens* strain GV3101::pMP90 by electroporation.

List of primers:

Primer name	Sequence	Used to generate
RLP4_GW_F	GGGGACAAGTTTGTACAAAAAAGCAGGCTTCACCATGATGCTTCGATTTATCCTAGCTTCTCTTCTC	pUBQ10::RLP4–RFP pUBQ10::RLP4-ECD–RFP
RLP4_GW_R	GGGGACCACTTTGTACAAGAAAGCTGGGTCAGACAACAAGCTCGGTCCATTTTCCAC	pUBQ10::RLP4–RFP pUBQ10::RLP4-ECD–RFP pRLP4::RLP4–GFP
RLP4L1_GW_F	GGGGACAAGTTTGTACAAAAAAGCAGGCTTCACCATGCCCTTCTCTCCTTCCTTCTTC	pUBQ10::RLP4-L1–RFP pUBQ10::RLP4-L1-ECD–RFP
RLP4L1_GW_R	GGGGACCACTTTGTACAAGAAAGCTGGGTCTTGCGAATTCAGTGGAAGAGTGGGC	pUBQ10::RLP4-L1–RFP pUBQ10::RLP4-L1-ECD–RFP pRLP4L1::RLP4-L1–GFP
RLP4_ECD_GW_R	GGGGACCACTTTGTACAAGAAAGCTGGGTCCTTGGCTCCAGAAGAAAGGTGAGGC	pUBQ10::RLP4-ECD–RFP
RLP4L1_ECD_GW_R	GGGGACCACTTTGTACAAGAAAGCTGGGTCTTTACCCCCTTTGGATAAG	pUBQ10::RLP4-L1-ECD–RFP
RLP4_pro_GW_F	GGGGACAAGTTTGTACAAAAAAGCAGGCTTCACCAATTTAAAACACCTAAGGAGTGCACATACGGTCGAGCTAGAGAAGAGTAGAG	pRLP4::RLP4–GFP
RLP4L1_pro_GW_F	GGGGACAAGTTTGTACAAAAAAGCAGGCTTCACCCTAAACAAAACTACCACGAGCTTAAGACTGAATGGAGAGGATAAGGAGAGGTG	pRLP4L1::RLP4-L1–GFP
secRFP_GW_F	GGGGACAAGTTTGTACAAAAAAGCAGGCTTCACCATGAAGACTAATCTTTTCTCTTTCTCATCTTTTCACTTCTC	pUBQ10::secRFP pUBQ10::secRFP–RLP4 pUBQ10::secRFP–RLP4-L1 pUBQ10::secRFP–RLP4ΔECD pUBQ10::secRFP–RLP4-L1ΔECD AtRPS5a»DEX»RLP4ΔECD AtRPS5a»DEX»RLP4-L1ΔECD
secRFP_GW_R_STOP	GGGGACCACTTTGTACAAGAAAGCTGGGTCTTAGGCGCCGGTGGAGTG	pUBQ10::secRFP
secRFP_R_LINKER	AGCTCCTCCAGCTCCTCCGGCGCCGGTGGAGTGGCG	pUBQ10::secRFP–RLP4 pUBQ10::secRFP–RLP4-L1 pUBQ10::secRFP–RLP4ΔECD pUBQ10::secRFP–RLP4-L1ΔECD AtRPS5a»DEX»RLP4ΔECD AtRPS5a»DEX»RLP4-L1ΔECD
RLP4_TMD_F_LINKER	GGAGGAGCTGGAGGAGCTATTGGCATTGCATTCGG	pUBQ10::secRFP–RLP4 pUBQ10::secRFP–RLP4ΔECD AtRPS5a»DEX»RLP4ΔECD

Primer name	Sequence	Used to generate
RLP4L1_TMD_F_LINKER	GGAGGAGCTGGA GGAGCTATAGCCA TAGCCATATC	pUBQ10::secRFP–RLP4-L1 pUBQ10::secRFP–RLP4-L1ΔECD AtRPS5a»DEX»RLP4-L1ΔECD
RLP44_GW_F	GGGGACAAGTTTG TACAAAAAAGCAG GCTTCACCATGAC AAGGAGTCACCG GTTAC	pUBQ10::RLP44–RFP
RLP44_GW_R	GGGGACCACTTTGT ACAAGAAAGCTGG GTCGTAATCAGGC ATAGATTGACTAATC TTACCTTC	pUBQ10::RLP44–RFP
RLP4_GW_R_STOP	GGGGACAAGTTTG TACAAAAAAGCAG GCTTCACCTCAAGA CAACAAGCTCGGTC	pUBQ10::secRFP–RLP4 pUBQ10::secRFP–RLP4ΔECD AtRPS5a»DEX»RLP4ΔECD
RLP4L1_GW_R_STOP	GGGGACAAGTTTGT ACAAAAAAGCAGG CTTCACCCTATTGC GAATTCAGTGGAAG AGTG	pUBQ10::secRFP–RLP4-L1 pUBQ10::secRFP–RLP4-L1ΔECD AtRPS5a»DEX»RLP4-L1ΔECD
RLP4_geno_CRISPR_F	GGATTAGTTGTGG AGCTAG	*rlp4 rlp4-l1* plant lines
RLP4_geno_CRISPR_F	TTGACTACTCCAA CCAGATT	*rlp4 rlp4-l1* plant lines
RLP4L1_geno_CRISPR_F	AAACTGAATTCTT CCTCTGTT	*rlp4 rlp4-l1* plant lines
RLP4L1_geno_CRISPR_R	ATCTCCAAGAGA AAACAAGAG	*rlp4 rlp4-l1* plant lines

Protein extraction and proteomics

Co-immunoprecipitation and mass spectrometry for the identification of interactors of YFP–RAB-A5c, YFP–RAB-A2a and YFP–RAB-G3f were performed as previously described[46]. In brief, the co-immunoprecipitation experiments were carried out by isolating total microsomes from *Arabidopsis* roots expressing YFP–RAB-A5c, YFP–RAB-A2a and YFP–RAB-G3f, or no transgene (Col-0). In-gel trypsin digest and mass spectrometry were performed by the Central Proteomic Facility, University of Oxford (www.proteomics.ox.ac.uk), and label-free quantification of the proteome was performed on three biological replicates using the SinQ pipeline[47]. We excluded all proteins that did not occur in all three replicates of YFP–RAB-A5c, replaced all remaining zero values in the matrix with the half-minimum value across all detected proteins and analysed the resulting 315 proteins for enrichment in RAB-A5c versus RAB-A2a and RAB-G3f proteomes using the Volcano plot function in the Perseus computational platform[48], with an S0 of 2 and FDR of 0.2, which identified 120 proteins significantly enriched in the YFP–RAB-A5c interactome compared with both YFP–RAB-A2a and YFP–RAB-G3f. We ranked these according to four criteria: (1) abundance in the YFP–RAB-A5c interactome (descending order), (2) relative enrichment against the YFP–RAB-A2a interactome (descending order), (3) relative enrichment against the YFP–RAB-G3f interactome (descending order) and (4) abundance in the Col-0 negative control (ascending order). We then assigned a super rank according to the sum of individual ranks in ascending order (Supplementary Data 1).

Microscopy and image analysis

Confocal microscopy was performed using a Zeiss 880 CLSM using a C-Apochromat ×40/1.20 W Corr M27 objective or a Zeiss 980 CLSM using a C-Apochromat ×40/1.20 W Corr M27 objective. GFP, YFP, RFP and PI were imaged as described before[23]. Image analysis and processing (orthogonal sectioning, maximum-intensity projections, image

assembly and quantification) were performed using Fiji v. 2.14.0 (ref. 49). For the quantification of colocalization between RLP4s–RFP and various endomembrane markers, CLSM stacks of lateral roots were subdivided in 25 μm × 25 μm substacks of meristematic epidermal cells. These areas were chosen to allow the assessment of tissue-scale differences in localization pattern as well as root-to-root differences. Background signal was removed using a hysteresis filter[49], using thresholds based on mean and minimum intensity minus 2 s.d. of ten randomly measured compartments for the respective CLSM channel, and Manders's colocalization coefficients[50] were determined using JACoP (Just Another Colocalisation Plugin) in Fiji v. 2.14.0 (ref. 51). Differences between different substacks from the same root were larger than differences between roots, and we pooled substacks from three or four lateral root stacks acquired during the same experiment. All experiments were conducted at least twice independently, and quantifications for one representative experiment are shown.

For the quantification of RLP4s–RFP at the PM, CLSM stacks of lateral roots co-expressing pUBQ10::YFP–NPSN12 and pUBQ10::RLP4s–RFP or pUBQ10::RLP44–RFP were collected at Nyquist resolution (voxel size, 99.5 nm × 99.5 nm × 550 nm). Midplane transverse and longitudinal sections of meristematic cells were generated in Fiji, and cellular outlines were manually traced using the PM marker YFP–NPSN12 as a reference. A plot profile with a width of seven pixels was generated, and RFP intensity was measured along the profile. The average signal intensity for ≥82 edges from meristematic epidermal cells of three or four lateral roots was calculated for 0.5-μm-wide intervals starting at the edge for longitudinal anticlinal, transverse anticlinal, longitudinal periclinal and transverse periclinal walls. The average intensity ± s.d. was plotted using the ggplot2 function in R Studio v. 4.1.2 (ref. 52). For the ablation experiments, 3D confocal stacks were acquired before and immediately after ablation. For quantitative analysis, only cell walls that were visibly deformed due to the ablation within a distance of six cells from the wound site were considered. RLP4–RFP and YFP–NPSN12 intensity along midplane sections of the same walls were quantified before and after ablation as described above, and the ratio post-/pre-ablation was calculated for each wall. The average ratio ± s.d. was plotted using the ggplot2 function in R Studio v. 4.1.2.

To quantify root thickness, we acquired bright-field images of lateral roots between 200 μm and 800 μm long and ensured that the mean root length was not significantly different across genotypes that were compared. The images were imported into Fiji v. 2.14.0, both sides of the root were traced manually along their longitudinal axis and *XY* Cartesian coordinates for each pixel on the outline trace were exported as .csv files and imported into RStudio v. 4.1.2 (https://www.rstudio.com/). For each pixel on one side, its closest neighbour on the other side was determined, and the Euclidian distance between pixels was calculated using the nn2 function in the RANN package (https://CRAN.R-project.org/package=RANN). The maximum diameter of each root was calculated as the average of the ten largest values excluding the tip-most 100 μm of each root to exclude the tapering tip. All experiments were conducted at least two times independently, and quantitative data from one representative experiment are shown.

Statistical data analysis and reproducibility

Two-way ANOVA was performed in R using the aov function from the stats package[53]. Tukey's test was performed in R using the TukeyHSD function from the stats package, and Student's *t*-test was performed in R using the t.test function from the stats package. The box, ribbon and violin plots were generated in R using the ggplot2 function[52]. In the box plots, the median is displayed as a horizontal line, the lower and upper edges correspond to the 25th and 75th percentiles, and the lower and upper whiskers extend from the edges to the smallest or largest value no further than 1.5× the interquartile range from the edge. Data beyond the ends of the whiskers are plotted individually. The violin plots show

the same information as the box plots, with the addition of the kernel probability density of the data at different values. The ribbon plots show the data mean ± s.d. (shaded areas).

All experiments were conducted at least twice and up to six times independently (see the details for specific experiments in the figure legends). For experiments involving confocal images of lateral roots, 3–8 lateral roots were imaged for each condition/genotype in each experimental repeat; for experiments involving bright-field images, 18–30 lateral roots were imaged in each experimental repeat. Data from one representative experiment are shown.

Reporting summary

Further information on research design is available in the Nature Portfolio Reporting Summary linked to this article.

Data availability

The data supporting the findings of this study are available within the Article and its Supplementary Information. The full proteomics dataset used in this study has been deposited at the PRIDE database under the title 'Comparative proteomic identification of Rab GTPase interactors in Arabidopsis', accession no. PXD044263. Source data are provided with this paper.

References

1. Cosgrove, D. J. Nanoscale structure, mechanics and growth of epidermal cell walls. *Curr. Opin. Plant Biol.* **46**, 77–86 (2018).
2. Carpita, N. C. & Gibeaut, D. M. Structural models of primary cell walls in flowering plants: consistency of molecular structure with the physical properties of the walls during growth. *Plant J.* **3**, 1–30 (1993).
3. Green, P. B. Mechanism for plant cellular morphogenesis. *Science* **138**, 1404–1405 (1962).
4. Cosgrove, D. J. Re-constructing our models of cellulose and primary cell wall assembly. *Curr. Opin. Plant Biol.* **22**, 122–131 (2014).
5. Haas, K. T., Wightman, R., Meyerowitz, E. M. & Peaucelle, A. Pectin homogalacturonan nanofilament expansion drives morphogenesis in plant epidermal cells. *Science* **367**, 1003–1007 (2020).
6. Lin, W. et al. *Arabidopsis* pavement cell morphogenesis requires FERONIA binding to pectin for activation of ROP GTPase signaling. *Curr. Biol.* **32**, 497–507.e4 (2022).
7. Peaucelle, A., Wightman, R. & Hofte, H. The control of growth symmetry breaking in the *Arabidopsis* hypocotyl. *Curr. Biol.* **25**, 1746–1752 (2015).
8. Park, Y. B. & Cosgrove, D. J. A revised architecture of primary cell walls based on biomechanical changes induced by substrate-specific endoglucanases. *Plant Physiol.* **158**, 1933–1943 (2012).
9. Boisson-Dernier, A. et al. Disruption of the pollen-expressed FERONIA homologs ANXUR1 and ANXUR2 triggers pollen tube discharge. *Development* **136**, 3279–3288 (2009).
10. Decreux, A. & Messiaen, J. Wall-associated kinase WAK1 interacts with cell wall pectins in a calcium-induced conformation. *Plant Cell Physiol.* **46**, 268–278 (2005).
11. Deslauriers, S. D. & Larsen, P. B. FERONIA is a key modulator of brassinosteroid and ethylene responsiveness in *Arabidopsis* hypocotyls. *Mol. Plant* **3**, 626–640 (2010).
12. Guo, H. et al. Three related receptor-like kinases are required for optimal cell elongation in *Arabidopsis thaliana*. *Proc. Natl Acad. Sci. USA* **106**, 7648–7653 (2009).
13. Hematy, K. et al. A receptor-like kinase mediates the response of *Arabidopsis* cells to the inhibition of cellulose synthesis. *Curr. Biol.* **17**, 922–931 (2007).
14. Lally, D., Ingmire, P., Tong, H.-Y. & He, Z.-H. Antisense expression of a cell wall–associated protein kinase, WAK4, inhibits cell elongation and alters morphology. *Plant Cell* **13**, 1317–1332 (2001).
15. Feng, W. et al. The FERONIA receptor kinase maintains cell-wall integrity during salt stress through Ca^{2+} signaling. *Curr. Biol.* **28**, 666–675.e5 (2018).
16. Kohorn, B. D. Cell wall-associated kinases and pectin perception. *J. Exp. Bot.* **67**, 489–494 (2016).
17. Ge, Z. et al. *Arabidopsis* pollen tube integrity and sperm release are regulated by RALF-mediated signaling. *Science* **358**, 1596–1600 (2017).
18. Gonneau, M. et al. Receptor kinase THESEUS1 is a Rapid Alkalinization Factor 34 receptor in *Arabidopsis*. *Curr. Biol.* **28**, 2452–2458 e4 (2018).
19. Haruta, M., Sabat, G., Stecker, K., Minkoff, B. B. & Sussman, M. R. A peptide hormone and its receptor protein kinase regulate plant cell expansion. *Science* **343**, 408–411 (2014).
20. Dünser, K. et al. Extracellular matrix sensing by FERONIA and leucine-rich repeat extensins controls vacuolar expansion during cellular elongation in *Arabidopsis thaliana*. *EMBO J. Online* **38**, e100353 (2019).
21. Kirchhelle, C. et al. The specification of geometric edges by a plant Rab GTPase is an essential cell-patterning principle during organogenesis in *Arabidopsis*. *Dev. Cell* **36**, 386–400 (2016).
22. Geldner, N. et al. Rapid, combinatorial analysis of membrane compartments in intact plants with a multicolor marker set. *Plant J.* **59**, 169–178 (2009).
23. Chow, C. M., Neto, H., Foucart, C. & Moore, I. Rab-A2 and Rab-A3 GTPases define a trans-Golgi endosomal membrane domain in *Arabidopsis* that contributes substantially to the cell plate. *Plant Cell* **20**, 101–123 (2008).
24. Wang, G. et al. A genome-wide functional investigation into the roles of receptor-like proteins in *Arabidopsis*. *Plant Physiol.* **147**, 503–517 (2008).
25. Wolf, S. et al. A receptor-like protein mediates the response to pectin modification by activating brassinosteroid signaling. *Proc. Natl Acad. Sci. USA* **111**, 15261–15266 (2014).
26. Wolf, S. Cell wall signaling in plant development and defense. *Annu. Rev. Plant Biol.* **73**, 323–353 (2022).
27. Adamowski, M. et al. A functional study of AUXILIN-LIKE1 and 2, two putative clathrin uncoating factors in *Arabidopsis*. *Plant Cell* **30**, 700–716 (2018).
28. Desprez, T. et al. Resistance against herbicide isoxaben and cellulose deficiency caused by distinct mutations in same cellulose synthase isoform CESA6. *Plant Physiol.* **128**, 482–490 (2002).
29. Gutierrez, R., Lindeboom, J. J., Paredez, A. R., Emons, A. M. C. & Ehrhardt, D. W. *Arabidopsis* cortical microtubules position cellulose synthase delivery to the plasma membrane and interact with cellulose synthase trafficking compartments. *Nat. Cell Biol.* **11**, 797–806 (2009).
30. Scheible, W. R., Eshed, R., Richmond, T., Delmer, D. & Somerville, C. Modifications of cellulose synthase confer resistance to isoxaben and thiazolidinone herbicides in *Arabidopsis* Ixr1 mutants. *Proc. Natl Acad. Sci. USA* **98**, 10079–10084 (2001).
31. Robert, S. et al. An *Arabidopsis* endo-1,4-beta-D-glucanase involved in cellulose synthesis undergoes regulated intracellular cycling. *Plant Cell* **17**, 3378–3389 (2005).
32. Hamant, O. et al. Developmental patterning by mechanical signals in *Arabidopsis*. *Science* **322**, 1650–1655 (2008).
33. Kirchhelle, C., Garcia-Gonzalez, D., Irani, N. G., Jérusalem, A. & Moore, I. Two mechanisms regulate directional cell growth in *Arabidopsis* lateral roots. *eLife* **8**, e47988 (2019).
34. Samalova, M., Kirchhelle, C. & Moore, I. Universal methods for transgene induction using the dexamethasone-inducible transcription activation system pOp6/LhGR in *Arabidopsis* and other plant species. *Curr. Protoc. Plant Biol.* **4**, e20089 (2019).
35. Hervieux, N. et al. A mechanical feedback restricts sepal growth and shape in *Arabidopsis*. *Curr. Biol.* **26**, 1019–1028 (2016).

36. Ambrose, C., Allard, J. F., Cytrynbaum, E. N. & Wasteneys, G. O. A CLASP-modulated cell edge barrier mechanism drives cell-wide cortical microtubule organization in *Arabidopsis*. *Nat. Commun.* **2**, 430 (2011).

37. Gust, A. A. & Felix, G. Receptor like proteins associate with SOBIR1-type of adaptors to form bimolecular receptor kinases. *Curr. Opin. Plant Biol.* **21**, 104–111 (2014).

38. Holzwart, E. et al. BRI1 controls vascular cell fate in the *Arabidopsis* root through RLP44 and phytosulfokine signaling. *Proc. Natl Acad. Sci. USA* **115**, 11838–11843 (2018).

39. Bosveld, F., Wang, Z. & Bellaïche, Y. Tricellular junctions: a hot corner of epithelial biology. *Curr. Opin. Cell Biol.* **54**, 80–88 (2018).

40. Dettmer, J., Hong-Hermesdorf, A., Stierhof, Y. D. & Schumacher, K. Vacuolar H+-ATPase activity is required for endocytic and secretory trafficking in *Arabidopsis*. *Plant Cell* **18**, 715–730 (2006).

41. Batoko, H., Zheng, H. Q., Hawes, C. & Moore, I. A Rab1 GTPase is required for transport between the endoplasmic reticulum and Golgi apparatus and for normal Golgi movement in plants. *Plant Cell* **12**, 2201–2217 (2000).

42. Wang, Z.-P. et al. Egg cell-specific promoter-controlled CRISPR/Cas9 efficiently generates homozygous mutants for multiple target genes in *Arabidopsis* in a single generation. *Genome Biol.* **16**, 144 (2015).

43. Clough, S. J. & Bent, A. F. Floral dip: a simplified method for *Agrobacterium*-mediated transformation of *Arabidopsis thaliana*. *Plant J.* **16**, 735–743 (1998).

44. Moore, I., Samalova, M. & Kurup, S. Transactivated and chemically inducible gene expression in plants. *Plant J.* **45**, 651–683 (2006).

45. Grefen, C. et al. A ubiquitin-10 promoter-based vector set for fluorescent protein tagging facilitates temporal stability and native protein distribution in transient and stable expression studies. *Plant J.* **64**, 355–365 (2010).

46. Kalde, M. et al. Interactions between Transport Protein Particle (TRAPP) complexes and Rab GTPases in *Arabidopsis*. *Plant J.* **100**, 279–297 (2019).

47. Trudgian, D. C. et al. Comparative evaluation of label-free SINQ normalized spectral index quantitation in the central proteomics facilities pipeline. *Proteomics* **11**, 2790–2797 (2011).

48. Tyanova, S. et al. The Perseus computational platform for comprehensive analysis of (prote)omics data. *Nat. Methods* **13**, 731–740 (2016).

49. Schindelin, J. et al. Fiji: an open-source platform for biological-image analysis. *Nat. Methods* **9**, 676–682 (2012).

50. Manders, E. M. M., Verbeek, F. J. & Aten, J. A. Measurement of co-localization of objects in dual-colour confocal images. *J. Microsc.* **169**, 375–382 (1993).

51. Bolte, S. & Cordelières, F. P. A guided tour into subcellular colocalization analysis in light microscopy. *J. Microsc.* **224**, 213–232 (2006).

52. Wickham, H. *ggplot2: Elegant Graphics for Data Analysis* (Springer, 2009); https://doi.org/10.1007/978-0-387-98141-3

53. R Core Team. R: A language and environment for statistical computing. R Foundation for Statistical Computing. https://www.R-project.org (2021).

Author contributions

L.E., I.M. and C.K. conceptualized the project. L.E., M.K., A.-K.S., X.Z. and C.K. devised the methodology. L.E., M.K. and A.-K.S. conducted the investigation. L.E. and C.K. created the figures. L.E., I.M. and C.K. acquired the funding. I.M. and C.K. administered the project. S.W., I.M. and C.K. supervised the project. L.E. and C.K. wrote the original draft of the paper. L.E., M.K., S.W. and C.K. reviewed and edited the manuscript.

Competing interests

The authors declare no competing interests.

Additional information

Extended data is available for this paper at https://doi.org/10.1038/s41477-024-01629-8.

Supplementary information The online version contains supplementary material available at https://doi.org/10.1038/s41477-024-01629-8.

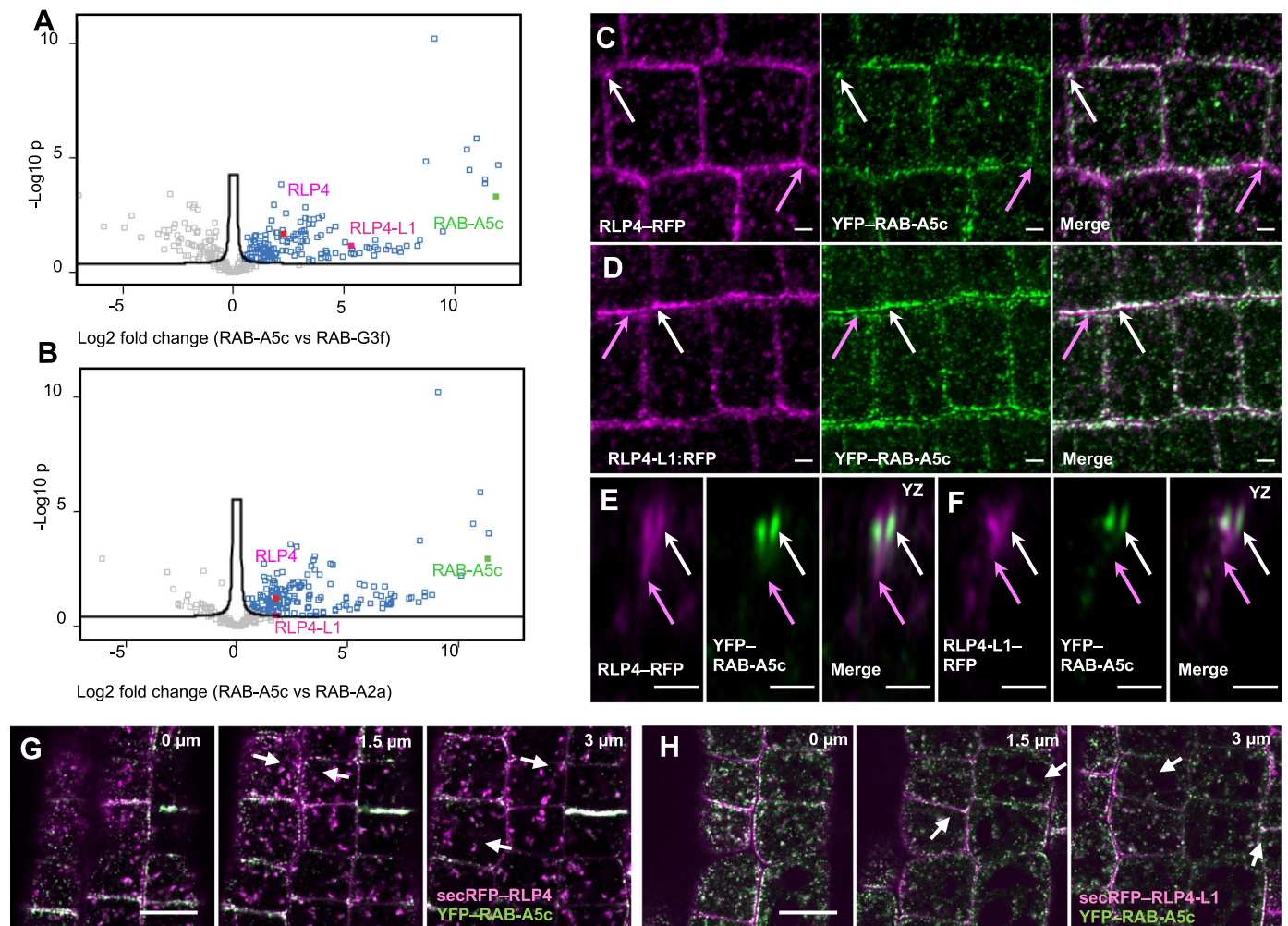**Correspondence and requests for materials** should be addressed to Charlotte Kirchhelle.

Peer review information *Nature Plants* thanks the anonymous reviewers for their contribution to the peer review of this work.

Reprints and permissions information is available at www.nature.com/reprints.

Publisher's note Springer Nature remains neutral with regard to jurisdictional claims in published maps and institutional affiliations.

Extended Data Fig. 1 | RLP4s contribute to directional growth control. (A,B) Volcano plots of the interactomes of YFP–RAB-A5c compared to YFP–RAB-G3f (A) and YFP–RAB-A2a (B). We conducted a two-sided volcano plot analysis with a S0 of 2 and FDR of 0.2 (non-adjusted for multiple comparisons), and proteins significantly enriched in the YFP–RAB-A5c interactome vs YFP–RAB-G3f or YFP–RAB-A2a in this analysis are colour-coded in blue. (C-F) CLSM maximum intensity (C,D) and YZ orthogonal projections (E,F) of lateral root epidermal meristem cells coexpressing *pRLP4s::RLP4s–RFP* (magenta) and *pRAB-A5c::YFP-RAB-A5c* (green). RLP4s–RFP colocalize with YFP–RAB-A5c at cell edge compartments (white arrows) and additionally label the peripheral cell edge (magenta arrows). Experiments were conducted at least 5 times independently, representative images are shown. (G,H) Sequential CLSM images of lateral root epidermal meristem cells co-expressing *pUBQ10::secRFP–RLP4s* (magenta) and *pRAB-A5c::YFP-RAB-A5c* (green). Experiments were conducted 3 times independently, representative images are shown. Scale bars 2 µm (C-F), 10 µm (G, H).
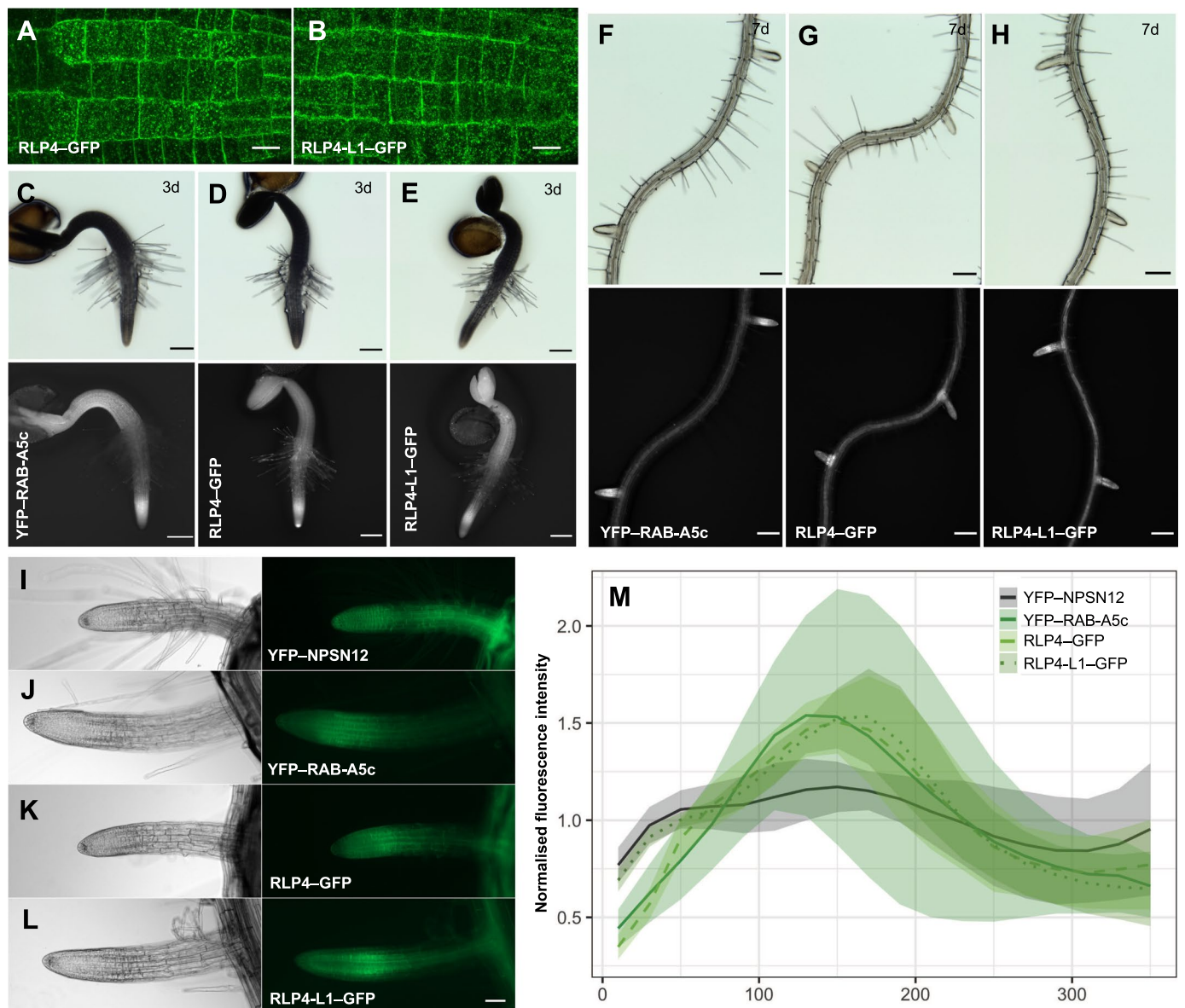
Extended Data Fig. 2 | Expression pattern of RLP4 and RLP4-L1. (A,B) CLSM maximum intensity projections of lateral root epidermal meristematic cells expressing *pRLP4s::RLP4s–GFP*. Experiments were conducted at least 5 times independently, representative images are shown. (C-L) Brightfield and wide-field fluorescent images of 3 day old seedlings (C-E), 10 day old roots (F-H), or lateral roots from 10d o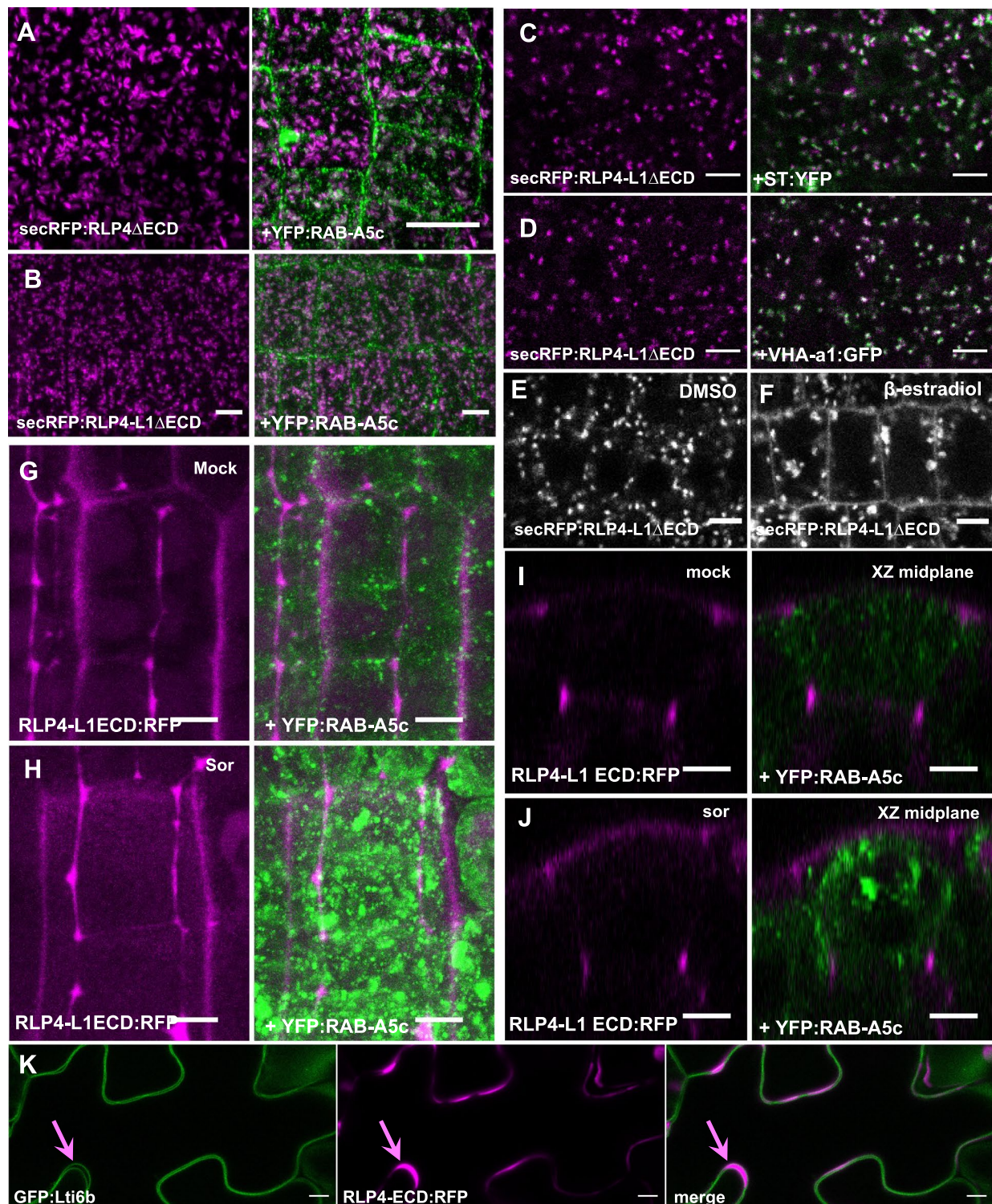ld plants (I-L) expressing *pUBQ10::YFP–NPSN12*, *pRAB-A5c::YFP–RAB-A5c*, *pRLP4::RLP4–GFP*, or *pRLP4-L1::RLP4-L1–GFP*. Experiments were conducted 3 times independently, representative images are shown. (M) Quantification of fluorescence intensity with increasing distance from the root tip in lateral roots such as those in (I-L). Plots are mean intensity +/- 1 SD. n = 11 (YFP–NPSN12, YFP–RAB-A5c,RLP4-L1–GFP), 13 (RLP4–GFP). Scale bars 10 µm (A,B), 50 µm (I-L) or 100 µm (C-H).
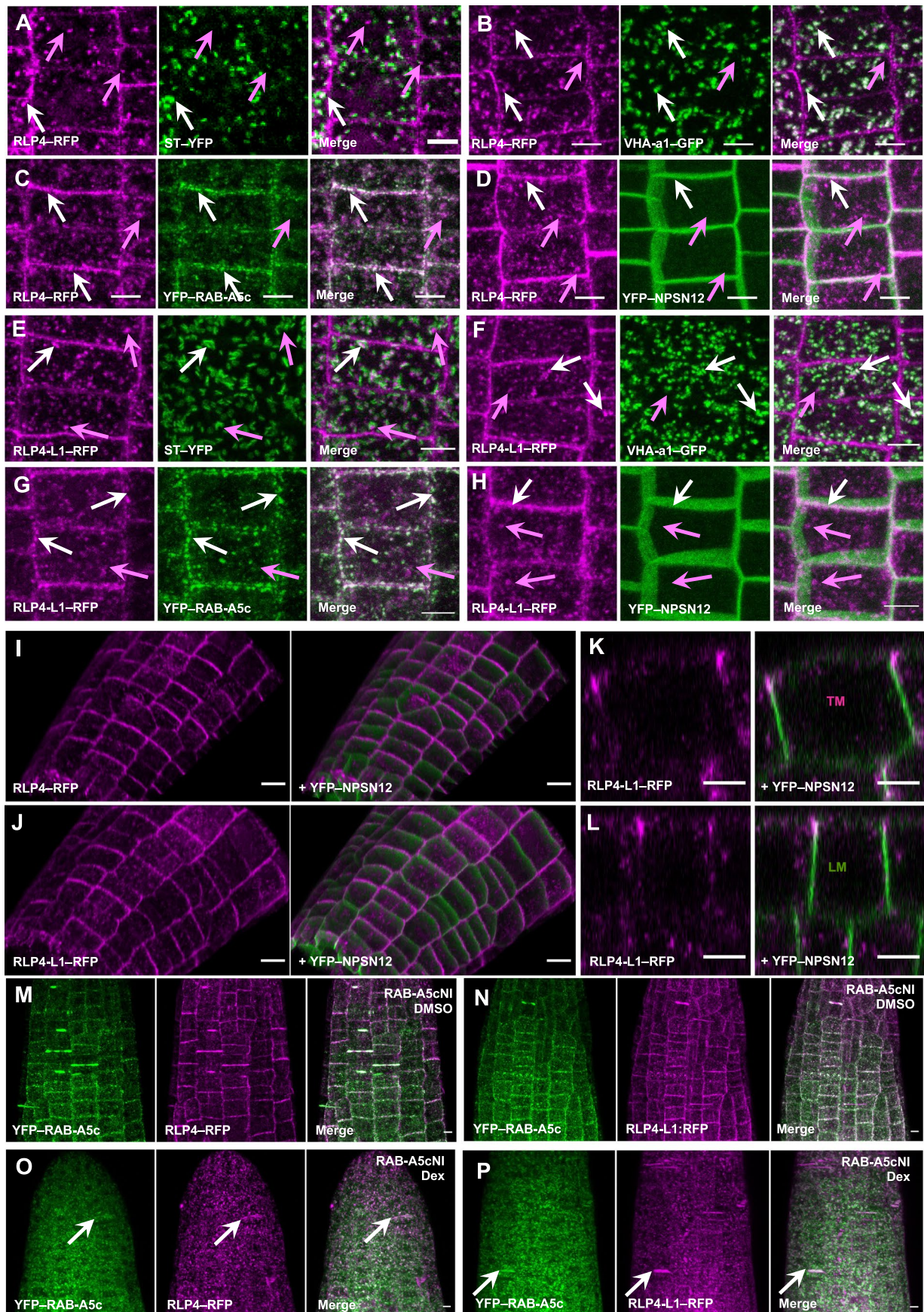
Extended Data Fig. 3 | See next page for caption.

Extended Data Fig. 3 | RLP4s are edge-restricted in Arabidopsis lateral root cells. (A-H) CSLM projections of lateral root epidermal meristem cells co-expressing pRLP4s::RLP4s–RFP or pUBQ10::RLP4s–RFP with various endomembrane markers. White arrows: colocalization of RLP4s–RFP with the respective endomembrane marker, magenta arrows: compartments uniquely labelled by RLP4s–RFP. Experiments were conducted 4 times independently, representative images are shown. (I,J) MorphoGraphX projections of lateral roots meristems co-expressing pUBQ10::RLP4s–RFP (magenta) and YFP–NPSN12 (green). Experiments were conducted at least 10 times independently, representative images are shown. (K,L) CLSM XZ/YZ projections representing transverse (TM; K) and longitudinal (LM; L) midplane sections through meristematic lateral root cells co-expressing pUBQ10::RLP4-L1–RFP (magenta) and YFP–NPSN12 (green). Experiments were conducted at least 10 times independently, representative images are shown. (M-P) CLSM maximum intensity projections of lateral root meristems co-expressing pUBQ10::RLP4s–RFP (magenta), YFP–RAB-A5c (green), and Dex-inducible dominant-negative AtRPS5a»DEX»RAB-A5c^{N125I} after 3d on DMSO (M,N) or 10 μM Dex (O,P). Arrows indicate cell plates. Experiments were conducted 2 times independently, representative images are shown. Scale bars 5 μm (A-H) or 10 μm (I-P).
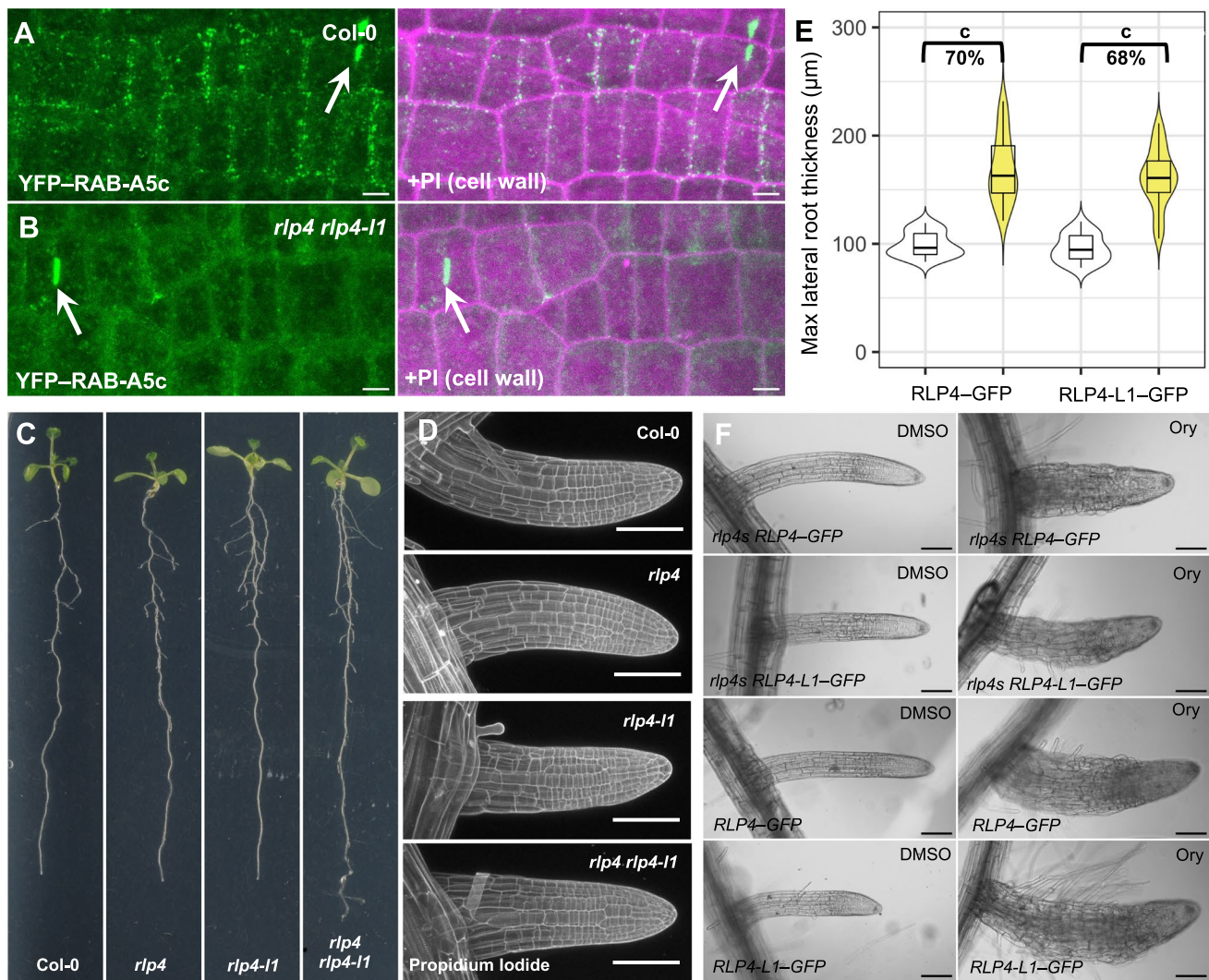
Extended Data Fig. 4 | RLP4s associate with the cell wall. (A,B) CLSM maximum intensity projections of lateral root epidermal meristem cells co-expressing pUBQ10::secRFP−RLP4sΔECD and YFP−RAB-A5c. Experiments were conducted 3 times independently, representative images are shown. (C,D) CLSM maximum intensity projections of lateral root epidermal meristem cells co-expressing *pUBQ10::secRFP−RLP4-L1ΔECD* with Golgi and TGN/EE markers. Experiments were conducted 3 times independently, representative images are shown. (E,F) CLSM of lateral roots co-expressing *pUBQ10::secRFP−RLP4-L1ΔECD* and β-estradiol-inducible A-L2 after 12 h treatment with DMSO or 10 μM β-estradiol. Experiments were conducted 3 times independently, representative images are shown. (G-J) CLSM maximum intensity or YZ orthogonal projections of lateral roots co-expressing *pUBQ10::RLP4-L1-ECD−RFP* and YFP−RAB-A5c after 30 minutes incubation in H_2O or 500 mM sorbitol. Experiments were conducted 3 times independently, representative images are shown. (K) CLSM single optical section of leaf epidermal pavement cells co-expressing *p35S::GFP−Lti6b* and *pUB10:RLP4-ECD−RFP*. Magenta arrow indicates RLP4-ECD−RFP localisation in the apoplast between plasma membranes of two cells labelled by GFP-Lti6b. Experiment was conducted 2 times independently, representative image is shown. Scale bars 5 μm.
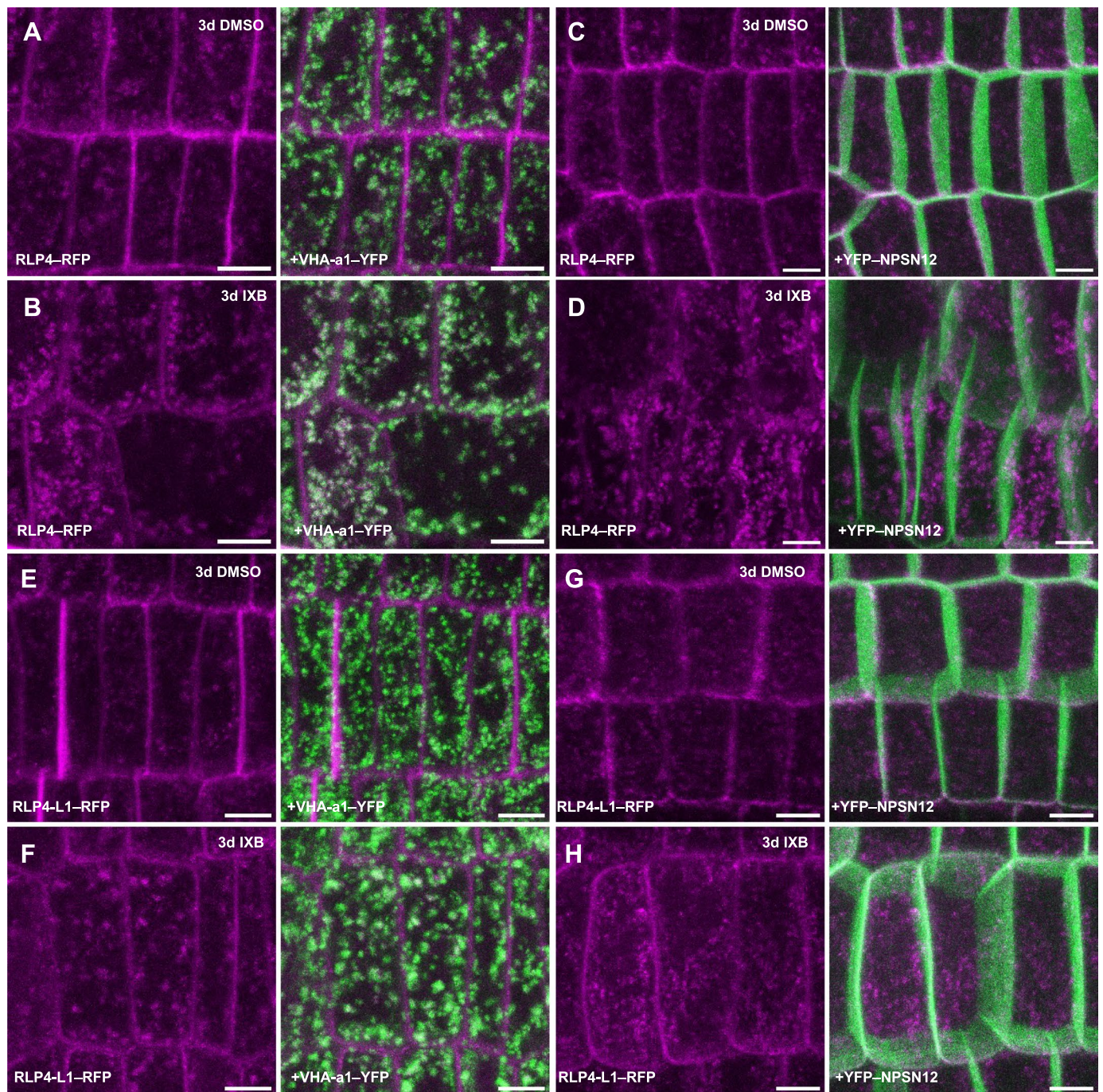
Extended Data Fig. 5 | RLP4s localization is sensitive to cell wall perturbation. (A-H) CLSM maximum intensity projections of lateral root epidermal meristematic cells co-expressing *pUBQ10::RLP4s–RFP* and VHA-a1–GFP (A,B,E,F) or YFP–NPSN12 (C,D,G,H) after 3d on plates containing 2.5 nM IXB (B,D,F,H) or an equivalent quantity of DMSO (A),C,E,G). Experiments were conducted 2 times independently, representative images are shown. Scale bars 5 μm.

Extended Data Fig. 6 | RLP4s are required for RAB-A5c localization. (A,B) CLSM maximum intensity projections of lateral root epidermal meristem cells expressing YFP–RAB-A5c in wild type (A) or *rlp4 rlp4-l1* (B) backgrounds. The cell wall was stained with propidium iodide. Cell plates are labelled with white arrows. Experiments were conducted 2 times independently, representative images are shown. (C) Photographs of 10d old Col-0, *rlp4*, *rlp4-l1*, and *rlp4 rlp4-l1* seedings. (D) CLSM maximum intensity projections of lateral roots from seedlings shown in (C). The cell wall was stained with propidium iodide. Experiments were conducted 2 times independently, representative images are shown. (E) Violin plots of the mean maximum diameter of lateral roots from plants after 3d treatment with DMSO or Oryzalin. N for plants treated with DMSO or Ory, respectively, was 32, 35 (*pRLP4::RLP4–GFP*) or 22, 37 (*pRLP4-L1::RLP4-L1–GFP*).

Difference in diameter (%) between DMSO (white) and Ory (yellow) treatments for each genotype noted above respective columns. Relative swelling in response to Ory is significantly increased compared to wild type plants (p = 0.005 and 0.028, respectively), but less so than in *rlp4 rlp4-l1* plants examined in the same experiment (Fig. 4G; p < 0.05, two-way ANOVA and post-hoc Tukey test). Experiment was conducted 3 times independently, and results from one representative experiment are shown. Violin plots are defined in the Methods section. (F) Representative images of lateral roots after 3d treatment with DMSO or Oryzalin from *rlp4 rlp4-l1 pRLP4::RLP4–GFP*, *rlp4 rlp4-l1 pRLP4-L1::RLP4-L1–GFP*, *pRLP4::RLP4–GFP*, *pRLP4-L1::RLP4-L1–GFP* plants as those in quantified in Fig. 4G, S6E. Experiments were conducted 3 times independently, representative images are shown. Scale bars 5 µm (A,B) or 100 µm (D,F).
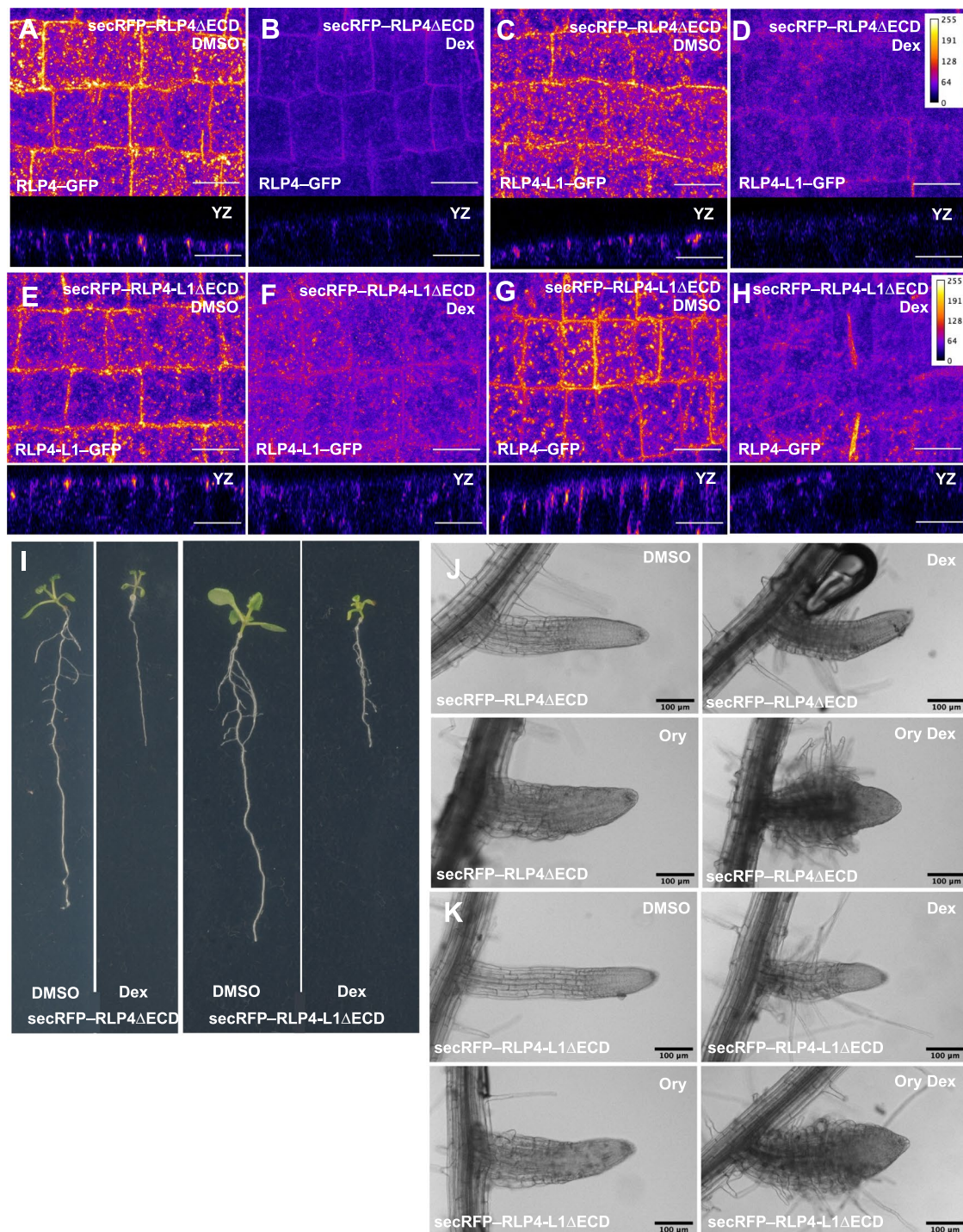
Extended Data Fig. 7 | RLP4s are involved in edge-based growth control. (A-H) CSLM maximum intensity projections or YZ projections of lateral root epidermal meristem cells co-expressing *pRLP4s::RLP4s–GFP* and *pUBQ10::secRFP–RLP4sΔECD* 72 hours after transfer to DMSO (A,C,E,G) or 10 μM Dex (B,D,F,H). Images are displayed in the ImageJ "fire" LUT to emphasize differences in intensity. Experiments were conducted 3 times independently, representative images are shown. (I) Photographs of 10d old *pRPS5a»Dex»secRFP–RLP4sΔECD*, seedlings grown on 0.1% DMSO (left) or 10 μM Dex (right). (J,K) Brightfield images of lateral roots expressing *AtRPS5a»DEX»secRFP–RLP4sΔECD* 3 days after transfer to DMSO, 500 nM Dex (A,B) or 1 μM Dex (C), 250 nM Ory, 500 nM Dex + 250 nM Ory (A,B), or 1 μM Dex + 250 nM Ory (C). Experiments were conducted 3 times independently, representative images are shown. Scale bars 10 μm (A-H) or 100 μm (J,K).

nature portfolio

Corresponding author(s): Charlotte Kirchhelle

Last updated by author(s): 25/07/2023

Reporting Summary

Nature Portfolio wishes to improve the reproducibility of the work that we publish. This form provides structure for consistency and transparency in reporting. For further information on Nature Portfolio policies, see our [Editorial Policies](#) and the [Editorial Policy Checklist](#).

Statistics

For all statistical analyses, confirm that the following items are present in the figure legend, table legend, main text, or Methods section.

n/a	Confirmed	
☐	☒	The exact sample size (n) for each experimental group/condition, given as a discrete number and unit of measurement
☐	☒	A statement on whether measurements were taken from distinct samples or whether the same sample was measured repeatedly
☐	☒	The statistical test(s) used AND whether they are one- or two-sided *Only common tests should be described solely by name; describe more complex techniques in the Methods section.*
☒	☐	A description of all covariates tested
☒	☐	A description of any assumptions or corrections, such as tests of normality and adjustment for multiple comparisons
☐	☒	A full description of the statistical parameters including central tendency (e.g. means) or other basic estimates (e.g. regression coefficient) AND variation (e.g. standard deviation) or associated estimates of uncertainty (e.g. confidence intervals)
☒	☐	For null hypothesis testing, the test statistic (e.g. F, t, r) with confidence intervals, effect sizes, degrees of freedom and P value noted *Give P values as exact values whenever suitable.*
☒	☐	For Bayesian analysis, information on the choice of priors and Markov chain Monte Carlo settings
☒	☐	For hierarchical and complex designs, identification of the appropriate level for tests and full reporting of outcomes
☒	☐	Estimates of effect sizes (e.g. Cohen's d, Pearson's r), indicating how they were calculated

Our web collection on [statistics for biologists](#) contains articles on many of the points above.

Software and code

Policy information about [availability of computer code](#)

Data collection	Confocal data were collected on a ZEISS 880 with the ZEN software (black edition) or a ZEISS 980 (ZEN 3.0).
Data analysis	We used the following published software and algorithms for data analysis: SinQ, Perseus 2.0.11, Fiji 1.0, R.Studio 2021.09.1+372 with the following packages: ggplot2, RANN, stats.

For manuscripts utilizing custom algorithms or software that are central to the research but not yet described in published literature, software must be made available to editors and reviewers. We strongly encourage code deposition in a community repository (e.g. GitHub). See the Nature Portfolio [guidelines for submitting code & software](#) for further information.

Data

Policy information about [availability of data](#)

All manuscripts must include a [data availability statement](#). This statement should provide the following information, where applicable:
- Accession codes, unique identifiers, or web links for publicly available datasets
- A description of any restrictions on data availability
- For clinical datasets or third party data, please ensure that the statement adheres to our [policy](#)

The authors confirm that the data supporting the findings of this study are available within the article and its supplementary materials. The full proteomics data set used in this study has been deposited at the PRIDE database under the title "Comparative proteomic identification of Rab GTPase interactors in Arabidopsis", accession PXD044263 (10.1038/S41467-023-41337-Z).

Research involving human participants, their data, or biological material

Policy information about studies with [human participants or human data](). See also policy information about [sex, gender (identity/presentation), and sexual orientation]() and [race, ethnicity and racism]().

Reporting on sex and gender	n/a
Reporting on race, ethnicity, or other socially relevant groupings	n/a
Population characteristics	n/a
Recruitment	n/a
Ethics oversight	n/a

Note that full information on the approval of the study protocol must also be provided in the manuscript.

Field-specific reporting

Please select the one below that is the best fit for your research. If you are not sure, read the appropriate sections before making your selection.

☒ Life sciences ☐ Behavioural & social sciences ☐ Ecological, evolutionary & environmental sciences

For a reference copy of the document with all sections, see nature.com/documents/nr-reporting-summary-flat.pdf

Life sciences study design

All studies must disclose on these points even when the disclosure is negative.

Sample size	Sample size was chosen such that difference levels would be detected with a power of 90% and a significance level of 5% based on control group parameters.
Data exclusions	We did not exclude data from our analyses.
Replication	All experiments presented in this paper were repeated independently at least two times, and were reproducible in all cases.
Randomization	For all treatments, plants were grown on shared agar plates and transferred to treatment conditions in even proportions, but without a random allocation sequence.
Blinding	The experimental work for this project was largely conducted by a single person (Liam Elliott, the lead author), who set up experiments and analysed data. Due to this setup, the experiments were not blinded.

Behavioural & social sciences study design

All studies must disclose on these points even when the disclosure is negative.

Study description	Briefly describe the study type including whether data are quantitative, qualitative, or mixed-methods (e.g. qualitative cross-sectional, quantitative experimental, mixed-methods case study).
Research sample	State the research sample (e.g. Harvard university undergraduates, villagers in rural India) and provide relevant demographic information (e.g. age, sex) and indicate whether the sample is representative. Provide a rationale for the study sample chosen. For studies involving existing datasets, please describe the dataset and source.
Sampling strategy	Describe the sampling procedure (e.g. random, snowball, stratified, convenience). Describe the statistical methods that were used to predetermine sample size OR if no sample-size calculation was performed, describe how sample sizes were chosen and provide a rationale for why these sample sizes are sufficient. For qualitative data, please indicate whether data saturation was considered, and what criteria were used to decide that no further sampling was needed.
Data collection	Provide details about the data collection procedure, including the instruments or devices used to record the data (e.g. pen and paper, computer, eye tracker, video or audio equipment) whether anyone was present besides the participant(s) and the researcher, and whether the researcher was blind to experimental condition and/or the study hypothesis during data collection.
Timing	Indicate the start and stop dates of data collection. If there is a gap between collection periods, state the dates for each sample cohort.

Data exclusions	*If no data were excluded from the analyses, state so OR if data were excluded, provide the exact number of exclusions and the rationale behind them, indicating whether exclusion criteria were pre-established.*
Non-participation	*State how many participants dropped out/declined participation and the reason(s) given OR provide response rate OR state that no participants dropped out/declined participation.*
Randomization	*If participants were not allocated into experimental groups, state so OR describe how participants were allocated to groups, and if allocation was not random, describe how covariates were controlled.*

Ecological, evolutionary & environmental sciences study design

All studies must disclose on these points even when the disclosure is negative.

Study description	*Briefly describe the study. For quantitative data include treatment factors and interactions, design structure (e.g. factorial, nested, hierarchical), nature and number of experimental units and replicates.*
Research sample	*Describe the research sample (e.g. a group of tagged Passer domesticus, all Stenocereus thurberi within Organ Pipe Cactus National Monument), and provide a rationale for the sample choice. When relevant, describe the organism taxa, source, sex, age range and any manipulations. State what population the sample is meant to represent when applicable. For studies involving existing datasets, describe the data and its source.*
Sampling strategy	*Note the sampling procedure. Describe the statistical methods that were used to predetermine sample size OR if no sample-size calculation was performed, describe how sample sizes were chosen and provide a rationale for why these sample sizes are sufficient.*
Data collection	*Describe the data collection procedure, including who recorded the data and how.*
Timing and spatial scale	*Indicate the start and stop dates of data collection, noting the frequency and periodicity of sampling and providing a rationale for these choices. If there is a gap between collection periods, state the dates for each sample cohort. Specify the spatial scale from which the data are taken*
Data exclusions	*If no data were excluded from the analyses, state so OR if data were excluded, describe the exclusions and the rationale behind them, indicating whether exclusion criteria were pre-established.*
Reproducibility	*Describe the measures taken to verify the reproducibility of experimental findings. For each experiment, note whether any attempts to repeat the experiment failed OR state that all attempts to repeat the experiment were successful.*
Randomization	*Describe how samples/organisms/participants were allocated into groups. If allocation was not random, describe how covariates were controlled. If this is not relevant to your study, explain why.*
Blinding	*Describe the extent of blinding used during data acquisition and analysis. If blinding was not possible, describe why OR explain why blinding was not relevant to your study.*

Did the study involve field work? ☐ Yes ☐ No

Field work, collection and transport

Field conditions	*Describe the study conditions for field work, providing relevant parameters (e.g. temperature, rainfall).*
Location	*State the location of the sampling or experiment, providing relevant parameters (e.g. latitude and longitude, elevation, water depth).*
Access & import/export	*Describe the efforts you have made to access habitats and to collect and import/export your samples in a responsible manner and in compliance with local, national and international laws, noting any permits that were obtained (give the name of the issuing authority, the date of issue, and any identifying information).*
Disturbance	*Describe any disturbance caused by the study and how it was minimized.*

Reporting for specific materials, systems and methods

We require information from authors about some types of materials, experimental systems and methods used in many studies. Here, indicate whether each material, system or method listed is relevant to your study. If you are not sure if a list item applies to your research, read the appropriate section before selecting a response.

Materials & experimental systems

n/a	Involved in the study
☒ ☐	Antibodies
☒ ☐	Eukaryotic cell lines
☒ ☐	Palaeontology and archaeology
☒ ☐	Animals and other organisms
☒ ☐	Clinical data
☒ ☐	Dual use research of concern
☐ ☒	Plants

Methods

n/a	Involved in the study
☒ ☐	ChIP-seq
☒ ☐	Flow cytometry
☒ ☐	MRI-based neuroimaging

Antibodies

Antibodies used	*Describe all antibodies used in the study; as applicable, provide supplier name, catalog number, clone name, and lot number.*
Validation	*Describe the validation of each primary antibody for the species and application, noting any validation statements on the manufacturer's website, relevant citations, antibody profiles in online databases, or data provided in the manuscript.*

Eukaryotic cell lines

Policy information about cell lines and Sex and Gender in Research

Cell line source(s)	*State the source of each cell line used and the sex of all primary cell lines and cells derived from human participants or vertebrate models.*
Authentication	*Describe the authentication procedures for each cell line used OR declare that none of the cell lines used were authenticated.*
Mycoplasma contamination	*Confirm that all cell lines tested negative for mycoplasma contamination OR describe the results of the testing for mycoplasma contamination OR declare that the cell lines were not tested for mycoplasma contamination.*
Commonly misidentified lines (See ICLAC register)	*Name any commonly misidentified cell lines used in the study and provide a rationale for their use.*

Palaeontology and Archaeology

Specimen provenance	*Provide provenance information for specimens and describe permits that were obtained for the work (including the name of the issuing authority, the date of issue, and any identifying information). Permits should encompass collection and, where applicable, export.*
Specimen deposition	*Indicate where the specimens have been deposited to permit free access by other researchers.*
Dating methods	*If new dates are provided, describe how they were obtained (e.g. collection, storage, sample pretreatment and measurement), where they were obtained (i.e. lab name), the calibration program and the protocol for quality assurance OR state that no new dates are provided.*

☐ Tick this box to confirm that the raw and calibrated dates are available in the paper or in Supplementary Information.

Ethics oversight	*Identify the organization(s) that approved or provided guidance on the study protocol, OR state that no ethical approval or guidance was required and explain why not.*

Note that full information on the approval of the study protocol must also be provided in the manuscript.

Animals and other research organisms

Policy information about studies involving animals; ARRIVE guidelines recommended for reporting animal research, and Sex and Gender in Research

Laboratory animals	*For laboratory animals, report species, strain and age OR state that the study did not involve laboratory animals.*
Wild animals	*Provide details on animals observed in or captured in the field; report species and age where possible. Describe how animals were caught and transported and what happened to captive animals after the study (if killed, explain why and describe method; if released, say where and when) OR state that the study did not involve wild animals.*
Reporting on sex	*Indicate if findings apply to only one sex; describe whether sex was considered in study design, methods used for assigning sex. Provide data disaggregated for sex where this information has been collected in the source data as appropriate; provide overall*

numbers in this Reporting Summary. Please state if this information has not been collected. Report sex-based analyses where performed, justify reasons for lack of sex-based analysis.

Field-collected samples | *For laboratory work with field-collected samples, describe all relevant parameters such as housing, maintenance, temperature, photoperiod and end-of-experiment protocol OR state that the study did not involve samples collected from the field.*

Ethics oversight | *Identify the organization(s) that approved or provided guidance on the study protocol, OR state that no ethical approval or guidance was required and explain why not.*

Note that full information on the approval of the study protocol must also be provided in the manuscript.

Clinical data

Policy information about clinical studies
All manuscripts should comply with the ICMJE guidelines for publication of clinical research and a completed CONSORT checklist must be included with all submissions.

Clinical trial registration | *Provide the trial registration number from ClinicalTrials.gov or an equivalent agency.*

Study protocol | *Note where the full trial protocol can be accessed OR if not available, explain why.*

Data collection | *Describe the settings and locales of data collection, noting the time periods of recruitment and data collection.*

Outcomes | *Describe how you pre-defined primary and secondary outcome measures and how you assessed these measures.*

Dual use research of concern

Policy information about dual use research of concern

Hazards

Could the accidental, deliberate or reckless misuse of agents or technologies generated in the work, or the application of information presented in the manuscript, pose a threat to:

No | Yes
☒ ☐ Public health
☒ ☐ National security
☒ ☐ Crops and/or livestock
☒ ☐ Ecosystems
☒ ☐ Any other significant area

Experiments of concern

Does the work involve any of these experiments of concern:

No | Yes
☒ ☐ Demonstrate how to render a vaccine ineffective
☒ ☐ Confer resistance to therapeutically useful antibiotics or antiviral agents
☒ ☐ Enhance the virulence of a pathogen or render a nonpathogen virulent
☒ ☐ Increase transmissibility of a pathogen
☒ ☐ Alter the host range of a pathogen
☒ ☐ Enable evasion of diagnostic/detection modalities
☒ ☐ Enable the weaponization of a biological agent or toxin
☒ ☐ Any other potentially harmful combination of experiments and agents

Plants

Seed stocks | The following transgenic lines used in this study were published previously: pRAB-A5c::YFP:RAB-A5c (Kirchhelle et al. (2016), Dev Cell 36, 386–400), AtRPS5a>Dex>RAB-A5c[N125I] (Kirchhelle et al. (2016), Dev Cell 36, 386–400), pUBQ10::YFP:NPSN12 (Geldner et al. (2009), Plant J 59, 169–178), pUBQ10::YFP:RAB-G3f (Geldner et al. (2009), Plant J 59, 169–178), pRAB:A2a::YFP:RAB-A2a (Chow et al. (2008), Plant Cell 20, 101–123) pVHA-a1::VHA-a1:GFP (Dettmer et al., Plant Cell 18, 715–730), p35S::ST:YFP (Batoko et al., Plant Cell 12, 2201–2217) and XVE>>AL1/XVE>>AL2 (Adamowski et al., Plant Cell 30, 700–716).

Novel plant genotypes | For the simultaneous targeting of RLP4 and RLP4-L1 via CRISPR/Cas9, two suitable sequences for the generation of guide RNAs were determined using the ChopChop webpage (https://chopchop.cbu.uib.no/) and incorporated into oligonucleotides that also contained

Eco31I recognition site at the 5' end and pHEE2E-TRI-specific1 sequence at the 3' end. pHEE2E-TRI was used as template to amplify the two targeting sequences together with promoter and terminator regions. The amplified PCR product was gel purified and ligated into Eco31I (BsaI)-digested pHEE2E-TRI. The assembled construct was mobilised in Agrobacterium tumefaciens strain GV3101 and used to transform Col-0 plants. T1 plants were selected on ½ MS, 0.75 % phytoagar and 15 μg/mL hygromycin. Plates were covered with sheets of paper for four to six days until positive T1 plants with an elongated hypocotyl could be distinguished and kept for another four days at full light. Around 40 T1 plants were transferred to soil and analysed for mutations using primers. We isolated a Cas9-free double mutant with single base insertions in both genes (position 264 from ATG for RLP4, position 363 for RLP4-L1), leading to premature stop codons 14 and 11 exons downstream, respectively.

To generate fluorescently tagged protein variants, target genes were amplified by PCR using PhusionTM High-Fidelity DNA Polymerase (Thermo Fisher Scientific) from gDNA isolated from Arabidopsis thaliana ecotype Columbia-0. pUBQ10::RLP4/4-L1:RFP, pUBQ10::RLP44:RFP, pUQ10B::RLP4/4-L1-ECD:RFP and pUB::RLP4/4-L1ΔID:RFP were all generated by cloning the relevant gDNA region into pDONR207 (Invitrogen/Thermo Fisher Scientific) using GatewayTM BP Clonase II Enzyme Mix (Thermo Fisher Scientific) and subsequently into pUB-RFP-DEST (9) using GatewayTM LR Clonase II Enzyme Mix (Thermo Fisher Scientific). For expression of RLP4:RFP and RLP4-L1:RFP from their native promoters, the UBQ10 promoter was removed from pUB-RFP-DEST through digestion with restriction endonucleases PspXI and PmeI (New England Biolabs) and the vector subsequently re-ligated using Klenow polymerase (DNA Polymerase I, Large fragment; New England Biolabs) and T4 DNA ligase (Thermo Fisher Scientific) to generate pX-DEST-RFP. The promoter region, 5'-UTR and coding region of RLP4 and RLP4-L were then amplified by PCR as single cassettes and cloned into pDONR207 and eventually pX-DEST-RFP as described above. To generate pUBQ10:secRFP:RLP4s and pUBQ10::secRFP:RLP4sΔECD, the relevant gDNA regions were overlapped with secRFP (Samalova et al., 2006) and the cassettes cloned into pENTR/D-TOPO using a pENTRTM/D-TOPOTM Cloning Kit (Thermo Fisher Scientific) and subsequently pUB-DEST44. For conditional expression of RLP4s and truncated variants using the pOp/LhGR system, transgenes were cloned into pDONR207 using GatewayTM BP Clonase II Enzyme Mix (Thermo Fisher Scientific) and subsequently into pOpIN2-RPS5a34 using GatewayTM LR Clonase II Enzyme Mix (Thermo Fisher Scientific). All constructs were verified by Sanger sequencing (Source Bioscience) and restriction digests. For molecular cloning, Escherichia coli strains DH5α and DB3.1 were used. For Agrobacterium-mediated transformation of Arabidopsis, constructs were introduced into Agrobacterium tumefaciens strain GV3101::pMP90 by electroporation.

Authentication	We examined phenotypes for all lines produced at the seedling and adult stage in comparison to wild type plants. Phenotypes oberserved included primary root length, plant height, and fertility. For fluorescent marker lines, we selected lines in which fluorescence segregated 3:1 in F2 populations, indicating a single insertion locus. All lines chosen were phenotypically indistinguishable from wild-type plants unless stated otherwise in the manuscript.

ChIP-seq

Data deposition

☐ Confirm that both raw and final processed data have been deposited in a public database such as GEO.

☐ Confirm that you have deposited or provided access to graph files (e.g. BED files) for the called peaks.

Data access links	For "Initial submission" or "Revised version" documents, provide reviewer access links. For your "Final submission" document,
May remain private before publication.	provide a link to the deposited data.
Files in database submission	Provide a list of all files available in the database submission.
Genome browser session (e.g. UCSC)	Provide a link to an anonymized genome browser session for "Initial submission" and "Revised version" documents only, to enable peer review. Write "no longer applicable" for "Final submission" documents.

Methodology

Replicates	Describe the experimental replicates, specifying number, type and replicate agreement.
Sequencing depth	Describe the sequencing depth for each experiment, providing the total number of reads, uniquely mapped reads, length of reads and whether they were paired- or single-end.
Antibodies	Describe the antibodies used for the ChIP-seq experiments; as applicable, provide supplier name, catalog number, clone name, and lot number.
Peak calling parameters	Specify the command line program and parameters used for read mapping and peak calling, including the ChIP, control and index files used.
Data quality	Describe the methods used to ensure data quality in full detail, including how many peaks are at FDR 5% and above 5-fold enrichment.
Software	Describe the software used to collect and analyze the ChIP-seq data. For custom code that has been deposited into a community repository, provide accession details.

Flow Cytometry

Plots

Confirm that:

☐ The axis labels state the marker and fluorochrome used (e.g. CD4-FITC).

☐ The axis scales are clearly visible. Include numbers along axes only for bottom left plot of group (a 'group' is an analysis of identical markers).

☐ All plots are contour plots with outliers or pseudocolor plots.

☐ A numerical value for number of cells or percentage (with statistics) is provided.

Methodology

Sample preparation	*Describe the sample preparation, detailing the biological source of the cells and any tissue processing steps used.*
Instrument	*Identify the instrument used for data collection, specifying make and model number.*
Software	*Describe the software used to collect and analyze the flow cytometry data. For custom code that has been deposited into a community repository, provide accession details.*
Cell population abundance	*Describe the abundance of the relevant cell populations within post-sort fractions, providing details on the purity of the samples and how it was determined.*
Gating strategy	*Describe the gating strategy used for all relevant experiments, specifying the preliminary FSC/SSC gates of the starting cell population, indicating where boundaries between "positive" and "negative" staining cell populations are defined.*

☐ Tick this box to confirm that a figure exemplifying the gating strategy is provided in the Supplementary Information.

Magnetic resonance imaging

Experimental design

Design type	*Indicate task or resting state; event-related or block design.*
Design specifications	*Specify the number of blocks, trials or experimental units per session and/or subject, and specify the length of each trial or block (if trials are blocked) and interval between trials.*
Behavioral performance measures	*State number and/or type of variables recorded (e.g. correct button press, response time) and what statistics were used to establish that the subjects were performing the task as expected (e.g. mean, range, and/or standard deviation across subjects).*

Acquisition

Imaging type(s)	*Specify: functional, structural, diffusion, perfusion.*
Field strength	*Specify in Tesla*
Sequence & imaging parameters	*Specify the pulse sequence type (gradient echo, spin echo, etc.), imaging type (EPI, spiral, etc.), field of view, matrix size, slice thickness, orientation and TE/TR/flip angle.*
Area of acquisition	*State whether a whole brain scan was used OR define the area of acquisition, describing how the region was determined.*

Diffusion MRI   ☐ Used   ☐ Not used

Preprocessing

Preprocessing software	*Provide detail on software version and revision number and on specific parameters (model/functions, brain extraction, segmentation, smoothing kernel size, etc.).*
Normalization	*If data were normalized/standardized, describe the approach(es): specify linear or non-linear and define image types used for transformation OR indicate that data were not normalized and explain rationale for lack of normalization.*
Normalization template	*Describe the template used for normalization/transformation, specifying subject space or group standardized space (e.g. original Talairach, MNI305, ICBM152) OR indicate that the data were not normalized.*
Noise and artifact removal	*Describe your procedure(s) for artifact and structured noise removal, specifying motion parameters, tissue signals and physiological signals (heart rate, respiration).*

Volume censoring	*Define your software and/or method and criteria for volume censoring, and state the extent of such censoring.*

Statistical modeling & inference

Model type and settings	*Specify type (mass univariate, multivariate, RSA, predictive, etc.) and describe essential details of the model at the first and second levels (e.g. fixed, random or mixed effects; drift or auto-correlation).*

Effect(s) tested	*Define precise effect in terms of the task or stimulus conditions instead of psychological concepts and indicate whether ANOVA or factorial designs were used.*

Specify type of analysis: ☐ Whole brain ☐ ROI-based ☐ Both

Statistic type for inference	*Specify voxel-wise or cluster-wise and report all relevant parameters for cluster-wise methods.*

(See Eklund et al. 2016)

Correction	*Describe the type of correction and how it is obtained for multiple comparisons (e.g. FWE, FDR, permutation or Monte Carlo).*

Models & analysis

n/a	Involved in the study
☐	☐ Functional and/or effective connectivity
☐	☐ Graph analysis
☐	☐ Multivariate modeling or predictive analysis

Functional and/or effective connectivity	*Report the measures of dependence used and the model details (e.g. Pearson correlation, partial correlation, mutual information).*

Graph analysis	*Report the dependent variable and connectivity measure, specifying weighted graph or binarized graph, subject- or group-level, and the global and/or node summaries used (e.g. clustering coefficient, efficiency, etc.).*

Multivariate modeling and predictive analysis	*Specify independent variables, features extraction and dimension reduction, model, training and evaluation metrics.*